

minimal changes to background elements or object appearances recontextualise events without triggering viewers. What makes these manipulations timely is their psychological effectiveness: our user study shows that even when explicitly instructed to look for AI-generated¹ content, human observers fail to identify FakeParts, with detection rates dropping by up to 26% vs full deepfakes.

This perceptual vulnerability creates a challenge in deepfake detection methods. Yet, current FakePart detection systems are not prepared to address this. This is mostly because no benchmark specifically targets these partial manipulations. While recent advances have enabled increasingly remarkable video manipulations—with models like Sora [12], VideoCrafter2 [18], and ModelScope [122] and specialized editing tools like ControlNet-like generation [47], video frame interpolation [57, 127, 129], camera control [51, 130, 134] and video inpainter [150, 161]—research on detection methods has lagged behind, primarily due to the lack of representative data. Specifically, deepfake detection research relies on very large-scale datasets with fully generated content or classic face-swaps [89, 92], creating a blind spot for more nuanced alterations.

To address this, we introduce FakePartsBench, the first large-scale benchmark designed to capture the full spectrum of partial deepfakes. It comprises over 81K videos, with 17K real, 20K full deepfakes and 44K FakeParts, which span diverse manipulations, from traditional face-swaps to state-of-the-art generative videos, with emphasis on partial edits, including localized inpainting, style transfer, object substitution, frame-specific edits and temporal interpolation. What distinguishes our dataset is its fine-grained annotation of manipulated regions, providing both pixel- and frame-level precision for evaluating FakeParts. Drawing from both public and private sources, FakePartsBench offers unprecedented diversity in content, context, and manipulation techniques (Figure 1).

Our comprehensive evaluation reveals alarming detection gaps for these localized manipulations. Through extensive human studies involving 290 participants, we demonstrate that FakeParts reduces human detection by up to 26% compared to full-video deepfakes, with certain categories such as interpolation and inpainting manipulations completely undetected. Similarly, state-of-the-art detectors show performance degradation of up to 50% when confronted with partial manipulations versus fully synthetic videos. Most concerning is the inverse relationship we discovered between manipulation subtlety and detection difficulty: the smallest edits often produce the most believable deceptions, precisely because they preserve maximum authentic context while changing critical semantic elements.

Our contributions are: (1) We define FakeParts as a novel and increasingly prevalent family of deepfakes dis-

tinguished by partial, localized manipulations within otherwise authentic video; (2) We present FakePartsBench, the first benchmark designed to capture partial deepfakes, featuring spatial and temporal manipulations; (3) Out extensive human and detection studies show detection gaps for partial manipulations, set baseline metrics and reveal critical areas for improvement. This work identifies a critical vulnerability in current detectors and provides the foundation for robust defenses against increasingly complex manipulations.

2. Related Work

Generation and Detection of Deepfake Image: Early detectors focused on low-level, hand-crafted inconsistencies such as copy-move, resampling, or sensor noise traces [21, 36, 53, 63, 125]. GANs [40] with large-scale training [11] enabled photorealistic faces, leading to detectors that cast the problem as binary classification [41, 84, 111, 145, 148]. However, such detectors often overfit to generators, training data, or image resolution [41, 123], and such brittleness is amplified for diffusion-generated images [9, 24, 25].

Recent detectors can be grouped into: (i) *Frequency-aware* detectors exploit persistent spectral artifacts [9, 76, 95, 100, 131, 154]. (ii) *Semantics-aware* approaches leverage robust representations from Large Vision-Language models (VLMs), e.g., CLIP [27, 90, 96, 149]. (iii) *Diffusion-specific* methods probe or invert the generative trajectory [82, 128]. Localisation-oriented methods such as FakeLocator [54] predict where manipulations occur in addition to classifying whether an image is fake.

We posit a unifying framework that places detectors along: a *detection-resolution axis* (pixel/patch \rightarrow image \rightarrow clip) and a *primary-cue axis* (frequency [54, 76, 95, 131], structural [26, 69, 107, 140], temporal [1, 20, 22, 48, 75, 85, 102, 104, 114, 132, 146], multimodal [37, 105, 121]). This explains the failures of single-scale, single-cue detectors against modern diffusion models and motivates patch-level processing for detecting partial edits.

Image Deepfake Datasets. Early datasets focused on GAN-generated faces [61], e.g., ForenSynths [123]. Subsequent corpora include DFDC [33], FaceForensics++ [101], WildDeepfake [160], and KoDF [67]. Recent ones target diffusion-generated images at scale, such as GenImage [159], DiffusionFace [19], and Deepfake-Eval-2024 [14] and face two issues: (1) they assume that edited regions are semantically dominant (e.g., full-face edits); and (2) only few provide fine-grained masks for small or blend-in edits. These motivate the shift to videos, where partial edits are more realistic and harder to detect.

Generation and Detection of Video Deepfakes: Early video forgeries primarily involve face swapping, i.e., Deepfakes mainly based on GANs [89, 106, 117–119, 137, 158]. Video detectors initially mirrored image-based strategies: framewise classifiers trained on real/fake clips [43, 72, 94,

¹In this work, we use *AI-Generated* and *deepfakes* interchangeably.

Dataset	Dur.(s)	Statistics				Realism			VBench Metrics			
		Real	Fake	Hi-Res	#Meth.	Cls-src.	FakeParts	FVD.W	FVD.FP	Cons.	Flick.	Qual.
GVD [81]	3	0	11,618	5,598	11	48	✗	387.7	549.7	0.932	0.968	0.656
VidProM [126]	3	0	6,690,00 ¹	30,000 ¹	4	0	✗	290.4	428.5	0.916	0.946	0.605
GenVidBench [88]	2	13,800	55,200	0	4	13,500 ²	✗	558.9	658.8	0.932	0.964	0.448
DeMamba [17]	4	10,000	8,588	2,156 ³	10	2,082	✗	382.8	459.7	0.934	0.967	0.651
FakePartsBench	5	17,252	64,252	≥24,365	21	12,000	✓	240.8	211.5	0.940	0.970	0.623

¹ VidProM Hi-Res comprises 30,000 videos at 720p from StreamingT2V, Open-Sora 1.2, and CogVideoX-2B. As it lacks a test set, we use these plus 10% randomly sampled from the training set.

² GenVidBench’s closed-source data are 560p at 24 fps, generated using Pika in 2022.

³ DeMamba’s Hi-Res includes 700 samples from MorphStudio, 1,400 from Lavie (both from 2023), and 56 videos from Sora.

Table 1. **Statistics of test sets of diffusion-based Deepfake Video Datasets.** FVD.W and FVD.FP denote FVD computed against WebVid-10M and our collected real dataset, respectively.

	Metadata			FakeParts		
	Name	Type	Venue	Spatial	Temporal	Style
GAN	ForgeryNet [52]	Face	CVPR’21	✓	✗	✗
	FakeAVCeleb [62]	F&V	NeurIPS’21	✓	✗	✗
	SWAN-DF [65]	F&V	IJCB’23	✓	✗	✗
	DiffSwap [152]	Face	CVPR’23	✓	✗	✗
	AV-Deepfake1M [13]	F&V	MM’24	✓	✗	✗
	DF40 [141]	Face	NeurIPS’24	✓	✗	✗
Diffusion	GVD [6]	Gen	PRCV’24	✗	✗	✗
	VidProM [126]	Gen	NeurIPS’24	✗	✗	✗
	GenVidBench [88]	Gen	arXiv’25	✗	✗	✗
	DeMamba [17]	Gen	arXiv’25	✗	✗	✗
	FakePartsBench (Ours)	Gen	2025	✓	✓	✓

Table 2. **Landscape of Deepfake Video Datasets.** F&V corresponds to Face & Voice and Gen to Generic videos, such as scenes, interior and exterior landscapes, cities, faces, etc.

[101, 151]. Temporal reasoning was later introduced through RNNs for dynamics [48] or segment localisation [85], and joint appearance-behaviour cues [1]. With diffusion-based video generators emerging [10, 12, 23, 157], newer detectors integrate semantic backbones and VLMs [81, 109], or spatio-temporal fusion such as optical flow [6]. Recent methods like DeMamba [17], built upon Mamba [42], show that long-range inconsistencies can be captured efficiently.

Within the aforementioned two-axis framework, these approaches extend the detection-resolution axis (frame \rightarrow clip) but remain sensitive to local cues such as lip-speech synchronisation [50, 147, 156]. Consequently, they struggle with *partial*, *short-span* manipulations, where only a few frames are altered and edits may not be facial.

Video Deepfake Datasets have evolved to large scale, e.g. FF++ video splits [101], DFDC [33], and DeeperForensics-1.0 [58], which target video face-manipulation under realistic capture and compression. Recent efforts aim at broader and newer forms of AI-generations: AV-Deepfake1M [13] scales to the audio-visual setting; DF40 [141] assesses detectors’ generalisation across unseen forgeries and domains; while the recent [78] targets multimodal deepfake detection for digital humans. In parallel, very recent datasets such

as VidProM [126], GenVidBench [88], GVD/AIVGDet [6], and DeMamba [17] explicitly explore T2V/I2V diffusion models, multimodal generation, and prompt configurations, making them suitable testbeds for fully synthetic videos.

These datasets exploit large-scale or multimodal generation [6, 88, 126] with optimized prompts [126]. Yet, they focus solely on fully synthetic videos (via T2V or I2V), omitting partially manipulated content (Table 2), and often lack modern high-resolution, high-quality samples (Table 1). These limitations not only limit progress towards robust detectors, but also fail to reflect real-world video forgery scenarios, which increasingly involve partial edits and content generated by high-quality proprietary models.

3. What is missing from Deepfake datasets?

Video Deepfake methods span a wide spectrum, not only in terms of underlying methodology (e.g., GAN [61, 89, 106, 117–119, 137, 158] vs. diffusion [10, 12, 23, 157]), but also in the nature of input conditions, such as text-to-video (T2V) [12, 18, 23, 157], image-to-video (I2V) [10, 47, 60], or a combination of both (TI2V) [12, 23]. They also differ in chromatic styling [133], spatial manipulation strategies, ranging from face swapping [92, 152] to regional inpainting [98] and outpainting [51, 130], as well as in temporal operations like frame interpolation [127].

To better understand the current landscape of video Deepfake datasets, we summarize key datasets in Table 2 and observe **one main limitation**:

- **Limitation 1: FakeParts.** Modern datasets lack videos with partial manipulations, referred to as FakeParts, which were prevalent during the GAN era but are now mostly absent from diffusion-based video benchmarks.

To evaluate recent *diffusion-based* datasets, we benchmark two key aspects:

- (i) **generation quality** through Fréchet Video Distance (FVD) [38] computed with respect to two real reference distributions: WebVid-10M [7] and our included Real data, each sampled 10,000 datapoints; and

(ii) **consistency, temporal flicker and image quality on VBench [55]**, corresponding to general video performance. Table 1 summarizes these results along with dataset statistics, including total duration, number of test samples, generation methods (#Method), high-resolution samples ($>720p$), and closed-source content. Details in the suppl. material. From Table 1, we observe the second limitation:

- **Limitation 2: Videos have low perceptual quality.** We observe a clear correlation between low resolution and low perceptual quality. For comparison, VidProM [126], which includes a higher proportion of high-resolution content, achieves significantly better FVD scores than other existing datasets.

4. FakePartsBench: A Benchmark for Video Deepfakes and FakeParts

In this work, we introduce FakePartsBench, a benchmark designed to address the two aforementioned limitations by

- incorporating a diverse and balanced mix of both full and partial manipulations (FakeParts);
- containing videos with high resolution and high quality. For this, we include videos generated by the latest open-source and closed-source models, such as Sora [12], Veo2 [23], and Allegro [157]. This ensures the timeliness and complementarity with existing benchmarks and also better reflects real-world scenarios, where an ever-growing share of Deepfake content online is produced by proprietary systems, often involving partial edits.

FakePartsBench supports research on detecting overt and covert forgeries. By combining large-scale coverage, high-resolution and fine-grained annotations, it enables rigorous evaluation. Next, we give statistics (Section 4.1), detail its generation pipeline (Section 4.2) and define FakeParts as:

(i) **Full Deepfakes** include entirely generated or heavily modified content, typically synthesized from a single input modality: e.g., text-to-video (T2V), or text-to-image-to-video (TI2V) (see Section 4.2.1 for details).

(ii) **FakeParts** include fine-grained manipulations that affect only specific aspects of a video. We further divide these into three subtypes (further elaborated in Section 4.2.1):

1. **Spatial FakeParts:** Manipulations on specific regions, e.g., face swapping (FaceSwap), object modification (inpainting), or contextual expansion (outpainting).
2. **Temporal FakeParts:** Edits along the temporal axis, e.g., frame interpolation.
3. **Style FakeParts:** Changes in visual appearance without altering structural content: e.g., modifying color schemes or applying different visual styles.

4.1. FakePartsBench Statistics

Table 3 reports statistics of FakePartsBench. It contains approximately 81K video clips, split into 17K real and **64K**

fake clips; hence, fake clips constitute more than 80% of the dataset, reflecting the broad coverage of edited and generative video categories represented.

FakePartsBench spans **9 tasks** from 21 distinct methods: *Style Change*, *Extrapolation*, *Faceswap*, *Inpainting*, *Interpolation*, *Outpainting*, *Real*, *T2V* (text-to-video), and *TI2V* (text-with-image-to-video). These tasks cover both traditional manipulation pipelines (e.g., Faceswap and Inpainting), modern generative video synthesis settings (T2V/TI2V) and novel partial-fake generation, including object colour editing and extrapolations. Resolutions range from 426×320 to 1920×1080 , frame rates from 50 to 30 FPS, and clip durations from 2 to 14 secs.

Importantly, FakePartsBench contains **>24K** high-resolution videos ($\geq 720p$), accounting for 30% of the dataset.

Figures 2-3 present statistics with respect to prompt length (measured by word count) and video content topics.

4.2. FakePartsBench generation process

FakePartsBench includes both real and fake videos; below, we outline their collection and generation processes, also illustrated in Figure 4. Figure 5 shows some examples.

Real videos. Many methods, particularly those involving partial manipulations, depend on real data. We use several publicly available datasets as real sources, including DAVIS 2016 [91], DAVIS 2017 [93], YouTube-VOS 2019 [142], MOSE [32] and LVD-2M [138]. The specific usage of each dataset per method is detailed in the suppl. material.

Vision-Language Models (VLMs). Many videos are captioned or evaluated using VLMs. Unless stated otherwise, we use PaLI-Gemma 2 (3B) fine-tuned on VQA_{v2} [110].

4.2.1. Full Deepfakes generation process

The Full Deepfake category includes two types:

First, **Text-to-Video (T2V)**, which includes various open-source (CogVideoX [144], Hunyuan Video [64], LTX-Video [49], Mochi 1 by Genmo [115], Open-Sora [153], Wan2.1 [120], AllegroAI [157]) and commercial (Sora [12], Veo2 [23]) generators published in 2024–2025. For all **T2V** methods, we generate diverse and semantically rich prompts using Google Gemini [116].

Second, **Text-and-Image-to-Video (IT2V)**, where we include the models that support dual-modals conditioning (text and image), i.e., Open-Sora [153], Wan2.1 [120]. We use the Gemini VLM: We extract the first frame from real videos (e.g., Pexels dataset [86]) and query Gemini to produce a continuation prompt based on it. We will include the prompts and conditioning frames in our metadata.

4.2.2. FakeParts generation process

I. Spatial FakeParts includes methods that alter regional information within the video content.

Task	#Meth.	Real V.	Fake V.	Total	Resolutions	FPS	Duration
Style Change [59, 66]	2	0	5,266	5,266	512×512; 680×384	8–10	2–14
Extrapolation [2, 34]	1	120,000	3,000	3,000	1280×704	25	5
Faceswap [29]	1	0	5,036	5,036	—	30	11
Inpainting [70, 136, 155]	3	7,252	13,577	20,829	426×320 to 1280×720	5–6	4–6
Interpolation [127]	1	0	10,000	10,000	512×320	7	7
Outpainting [130]	1	0	7,275	7,275	576×320	8	2
Real	1	10,000	0	10,000	640×360	30	6
T2V [49, 64, 115, 144] [12, 23, 120, 153, 157]	9	0	16,119	16,119	720×480 to 1920×1080	15–30	4–6
Text-to-Image-to-Video [120, 153]	2	0	3,980	3,980	720×1280; 1024×576	16–24	5
ALL	21	17,252	64,252	81,504	—	—	—

Table 3. Statistics and Quality of FakePartsBench Grouped by Task Category.

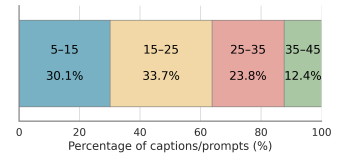


Figure 2. Prompt word-count.

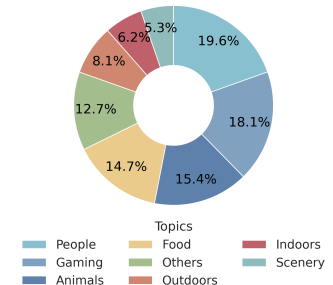


Figure 3. Prompt topic distribution.

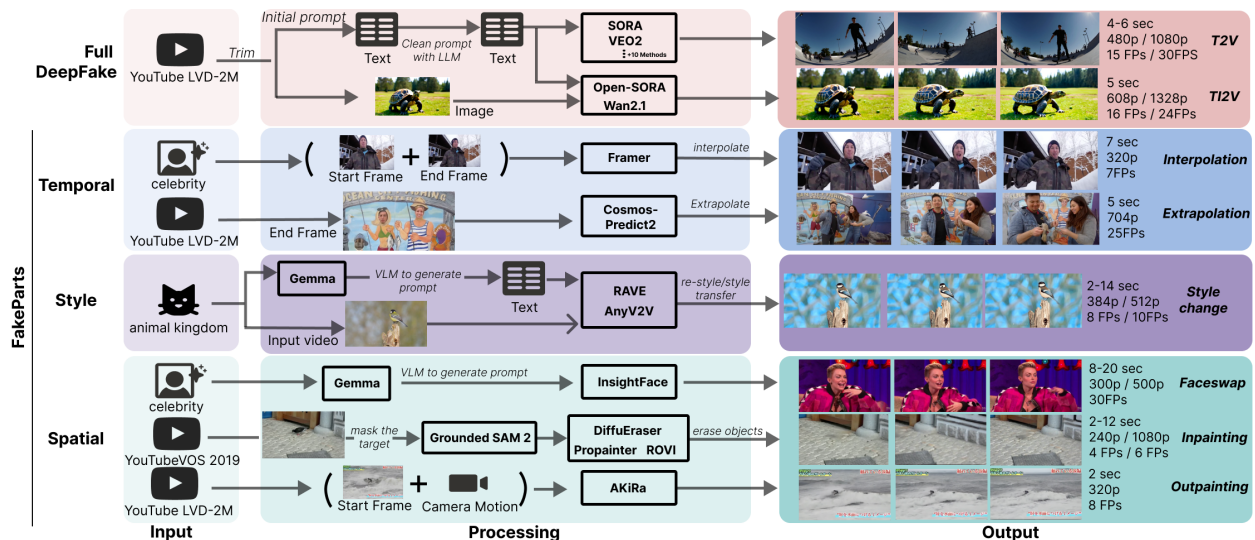


Figure 4. **Pipeline** of FakePartsBench includes both full and FakeParts Deepfake videos. The partial manipulations, FakeParts, are categorized into three types: temporal, spatial, and style.

Faceswap. We replace the face in a target video with that from a source face image. For this, we use the a widely used tool for face detection and swapping, InsightFace library [3, 4, 28–31, 39, 44, 45, 99]. During generation, we use target videos from the Celeb-DF dataset [73] and source images from CelebA [79] to avoid the misuse of sensitive facial information. Both datasets focus exclusively on celebrities, whose facial identities are already publicly exposed. To ensure gender consistency after swapping, we prompt VLM with gender and filter the unmatched pairs.

Inpainting Generation. We include two such sources. First, we generate inpainted videos using DiffuEraser [70] and ProPainter [155]. The pipeline consists of: (1) extracting the first frame and using a VLM to identify a salient ob-

ject to remove; (2) segmenting the object across all frames with Grounded-SAM-2 [97]; and (3) applying the inpainting models to remove the object and fill the masked regions, producing realistic object-removal deepfakes. Second, we include the inpainting dataset from ROVI [136], where videos are inpainted using E2FGVI [74] with careful human curation and parameter tuning.

Outpainting. Video outpainting accounts for camera motion and 3D consistency. Recent approaches address this through explicit camera control [51, 130, 134, 139]. We use AkiRA [130], built on SVD [10]. For generation, we apply backwards camera tracking trajectories to guide coherent extrapolation at frame boundaries.

II. Temporal FakeParts includes methods that complete or

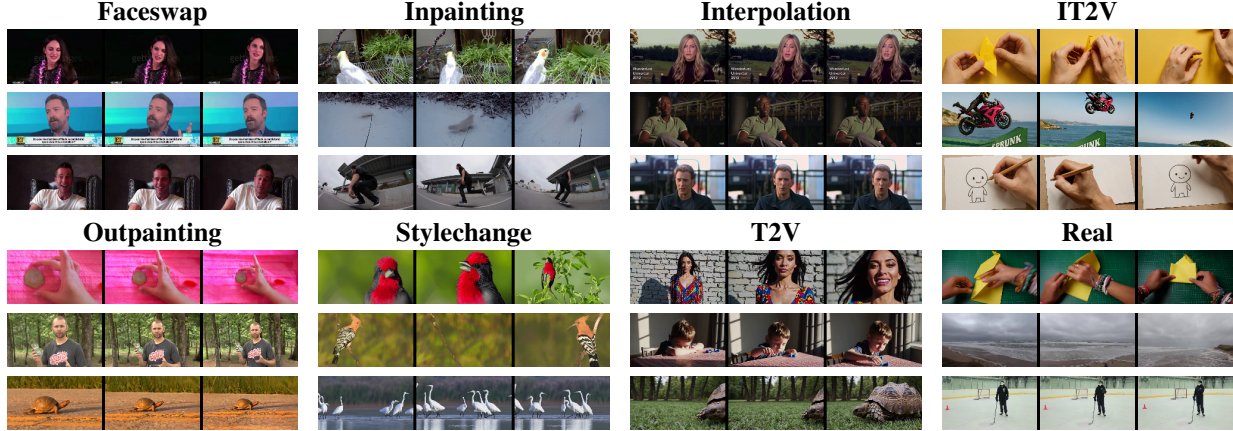


Figure 5. FakePartsexamples grouped by manipulation group (per column) with three samples per group.

Category	Method	Venue	C	Description
Out-of-the-box (OoB) CNN- or ViT-based binary detectors trained on their respective datasets	NPR [112]	CVPR'24	I	Focus on pixel-neighbour relations, local cues from upsampling, to capture general artefacts
	HiFi [46]	CVPR'23	I	Exploits hierarchical feature discrimination for GAN- and diffusion-generated images
	AIGVDet [6]	PRCV'24	V	Combines spatial and optical flow branches to detect frame-level inconsistencies, fused into robust video-level predictions
	CNNDetection [124]	CVPR'20	I	Trained on one generator (ProGAN), it generalizes by learning shared low-level artifacts
Foundation-Model-Based (FoM) detectors that leverage pretrained large-scale models (e.g., CLIP [96])	IML-ViT [83]	NeurIPS'24	I	ViT-based Image Manipulation Localization method using high-res, multi-scale features and edge supervision to capture subtle traces
	UnivFD [90]	CVPR'23	I	CLIP embeddings with linear probes or nearest neighbours to detect fakes from GANs, diffusion, and autoregressive models
	D3 [143]	CVPR'25	I	Dual-branch CLIP-with-attention method that detects discrepancy artefacts
	C2P-CLIP [113]	AAAI'25	I	CLIP-based detector that employs category-concept prompts
	FatFormer [77]	CVPR'24	I	CLIP backbone augmented with a forgery-aware adapter and prompt conditioning
VLM-Based (VLM) use prompt- or fine-tuned VLMs that output predictions (no confidence scores)	De-Fake [103]	ArXiv'23	I	CLIP-aligned detector that decouples real/fake evidence; improves open-set generalisation
	FakeVLM [135]	NeurIPS'25	I	MLLM specialised for synthetic-image detection with natural-language artefact explanations
	SIDA [56]	CVPR'25	I	Extends a VLM with special tokens to capture image-level authenticity cues, enabling classification of real, synthetic, and tampered images
Diffusion-Based (DiB) use denoising signals from pretrained DM	MM-Det [108]	NeurIPS'24	V	Integrates VLM (LLaVA) with spatio-temporal attention to detect diffusion-generated videos through joint visual-textual reasoning
	AntifakePrompt [15]	ArXiv'25	I	Prompt-tuned VLMs (InstructBLIP) cast as VQA; strong zero- and few-shot generalisation
DRCT [16]	ICML'24	I	Leverages contrastive training on diffusion-inverted reconstructions to distinguish fake content from real videos	

Table 4. **Forgery methods evaluated.** Column ‘C’ corresponds to image or video level category of method.

modify content along time axis, such as frame interpolation.

Interpolation Generation. We employ Framer [127] to synthesize smooth transitions between non-consecutive frames, simulating temporal edits. We randomly select 14 consecutive frames from each video, provide the first and last frames to Framer to generate 14 synthetic intermediate frames, and obtain a temporally edited video.

Extrapolation Generation. We employ the Cosmos Predict Video2World framework [2, 34, 35] to generate temporally extrapolated videos from real footage. Given the final 50 frames of a captured sequence with their caption as prompt, the model predicts and synthesizes the subsequent motion and scene evolution, extending each clip to 120 frames. The resulting videos of 25FPS and 5 seconds,

preserve the original scene context while introducing plausible forward dynamics, forming our extrapolation subset.

III. Style FakeParts targets manipulations that retain the semantic content of the video but modify its appearance through style transfer techniques.

Style Change Generation. We use RAVE [59] to alter color and appearance on videos from Animal Kingdom [87]. A random frame is captioned with PaLI-Gemma2 [110], and RAVE is prompted with: ‘Change the colour of the animal in the video.’ We also include object-specific colour edits using AnyV2V [66], where we caption frames using VideoChat-R1 [71], and then extract the object to be edited and pair it with target colour. The resulting prompt (‘Change the colour of the car to blue while keeping

Table 5. Performance comparison of video generators and detectors using % ROC-AUC (or equivalent) scores. Green cells indicate scores above 85%, while red cells denote scores below 53%.

Category	Gen vs. Det	Venue	IT2V	T2V	Interp.	Extrap.	Inpaint.	Outpaint.	Face	Style
-	Random	-	50.0	50.0	50.0	50.0	50.0	50.0	50.0	50.0
OoB	NPR [112]	CVPR24'	68.3	72.8	57.0	61.1	37.2	59.2	66.7	59.5
	HiFi [46]	CVPR23'	60.3	60.1	53.7	45.8	45.5	49.9	65.2	65.2
	AIGV [6]	PRCV24'	48.0	46.3	48.1	51.4	37.3	57.6	82.2	33.4
	CNNDet [124]	CVPR20'	55.5	94.8	54.0	62.3	67.8	57.4	45.9	66.1
	IML-ViT [83]	NeurIPS24'	32.8	61.2	57.2	45.3	56.0	44.1	58.2	34.0
FoM	UnivFD [90]	CVPR23'	65.0	89.1	65.9	58.1	83.1	57.9	58.4	83.5
	D3 [143]	CVPR25'	81.8	94.8	75.4	70.6	72.9	71.3	37.5	83.5
	C2P [113]	AAAI25'	83.1	96.5	88.9	84.3	68.3	82.2	60.6	88.1
	Fatfrm. [77]	CVPR24'	43.2	63.1	50.2	47.8	53.7	53.2	47.7	56.8
	De-Fake [103]	ArXiv23'	94.4	70.9	48.0	49.2	44.4	96.3	48.8	49.0
VLM	FakeVLM [135]	NeurIPS25'	46.3	47.2	50.6	50.4	46.4	51.3	46.2	54.3
	SIDA [56]	CVPR25'	83.9	52.6	47.2	46.3	34.5	47.3	62.3	25.4
	MM-Det [108]	NeurIPS24'	54.3	52.8	61.9	53.5	37.1	59.9	63.1	52.7
	AFPrompt [15]	ArXiv25'	50.0	50.0	50.0	50.0	50.0	50.0	50.0	50.0
DiB	DRCT [16]	ICML24'	72.0	86.0	97.2	44.6	70.9	95.2	71.9	96.4
-	Human	-	83.1	86.3	60.2	60.0	83.3	83.3	80.0	82.0

the rest of the scene unchanged.’) ensures only local edits.

5. Experimental Protocol

We benchmark state-of-the-art image and video detectors on FakePartsBench. Specifically, all detectors are grouped into four groups according to their underlying detection mechanisms, as explained in Table 4: **Out-of-the-box (OoB)**, **Foundation-Model-Based (FoM)**, **VLM-Based (VLM)**, and **Diffusion-Based (DiB)**.

Each video is decoded into full-resolution without any resizing, aspect-ratio normalisation, or geometric alignment. This ensures that the frames retain their original aspect ratio and any artefacts introduced during generation and preserves the native spatial characteristics of the data, allowing subsequent analysis on unaltered visual content rather than resized or warped patches.

5.1. Detection Performance

Table 5 reports the AUC-ROC scores per model, when available, given that some VLM-based detectors output direct binary predictions. Each row corresponds to a detector grouped into: **Out-of-the-Box (OoB)**, **Foundation-Model-Based (FoM)**, **Vision–Language–Model-Based (VLM)**, and **Diffusion-Based (DiB)**. Columns report detector performance across generator families, including **Full-Fake Generators (T2V and IT2V)** and **Fake-Part Generators (Change-of-Style, Inpainting, Outpainting, Interpolation, Extrapolation, and Faceswap)**. Figure 6 shows category-wise performances, aggregating the detectors within each category into radar plots that reveal consistent trends across generator types. We draw the following findings:

1. Full-fake content is comparatively easy to detect.

Across nearly all detectors, full-fakes such as *IT2V* and *T2V* are detected with relatively high and consistent score (more green cells in Table 5). For example, *T2V* videos, which contain no real frames, are detected by most FoM detectors, the diffusion-based detector (DiB), and even human raters at above 85% AUC. Interestingly, introducing only a *single real frame*, as in *IT2V*, already reduces performance compared to pure *T2V*: C2P [113] reduces 96.5% to 83.1% and DRCT [16] reduces from 86% to 72%. Moreover, detector performance drops substantially for FakeParts, as seen in the columns for *Inpaint.*, *Interp.*, and *Extrap.*. Many detectors exhibit weak performance (red cells), with some AUCs even falling below 50%, i.e., worse than random chance.

2. OoB and VLM-based detectors perform poorly.

OoB CNN/ViT-style detectors and VLM-based approaches often operate near or below random-chance accuracy, particularly on FakeParts generators such as *Inpaint.*. Although they occasionally achieve reasonable performance on certain full-fake settings; e.g., CNNDet [124] reaches 94.8% AUC on *T2V*, and SIDA [56] 83.9% on *IT2V*. Their behavior is unstable across manipulation types. Both drop to below ~65% AUC for nearly all other generator.

3. FoM detectors work well on full-fake content but are brittle on FakeParts.

FoM achieve strong performance on full-fake videos: *IT2V* (e.g., De-Fake [103] reaches 94.4%) and *T2V* (e.g., C2P [113] at 96.5%, D3 at 94.8%, UnivFD at 89.1%). However, their performance drops sharply on FakeParts manipulations such as *Inpaint.* (C2P at 68.3%), *Outpaint.* (Uni-

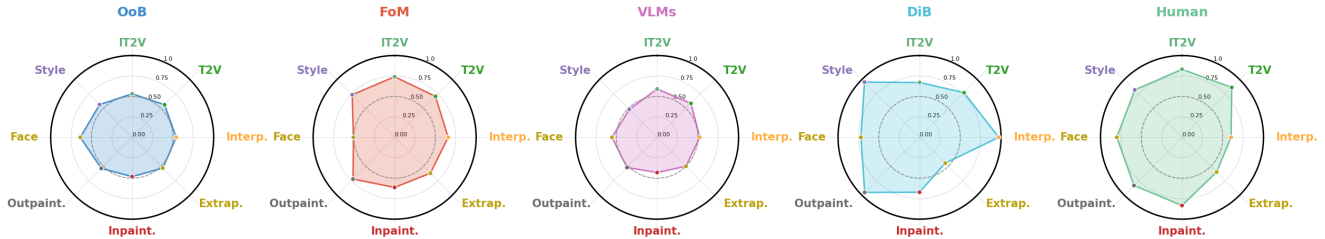


Figure 6. **Results** in Radar map of FakePartsBench performance across detector categories, where for each category we report the average performance achieved among all generators: **OoB**, **FoM**, **VLMs**, and **DiB** and on various generators, including **full fake** generators such as: **T2V**, **IT2V**, and FakeParts: **Change-of-Style**, **Inpainting**, **Outpainting**, **Interpolation**, **Extrapolation**, and **Faceswap**.

vFD at 57.9%), *Interp.* (De-Fake at only 48.0%), and *Face* (none of the FoM methods exceed 60%). Notably, most FoM detectors rely on CLIP and almost none handle inpainting, face swap, or extrapolation reliably, revealing a core weakness of current CLIP-based approaches.

4. Diffusion-based detection offers the best balance between accuracy and coverage.

Compared with others the diffusion-based model exhibits the most balanced performance profile in both Table 5 and Figure 6. It maintains strong accuracy across full-fake *IT2V* and *T2V* as well as across diverse FakeParts manipulations, with the only notable weakness being the extrapolation case (44.6%). Although it does not always achieve the single best score on every axis, its combination of high accuracy and broad robustness makes diffusion-based detection the most reliable category overall in our benchmark.

5. FakeParts impact human performance.

Comparing detector performance with human judgments reveals several informative parallels. Humans achieve their highest AUC (86.3%) on full-fake videos, particularly *T2V*, mirroring the performance trends observed in many detectors. For FakeParts manipulations, human evaluators remain relatively sensitive to *Inpaint.*, *Outpaint.*, and *Face*, typically achieving AUC values above 80%. However, they perform significantly worse on *Interp.* and *Extrap.*, both around 60%. We believe this pattern reflects inherent differences in human sensitivity to spatial versus temporal inconsistencies: spatial artifacts (e.g., inpainting) are easier to perceive, whereas temporal irregularities (e.g., interpolation) are harder to differentiate. Interestingly, while humans are often weaker than the top detectors on full-fake content, they remain the *most balanced and reliable* judges for FakeParts content, as shown on the right side of Figure 6. This further highlights the challenge that partial edits pose for current automated detection systems.

→ **Why do these patterns emerge?** We attribute the weaknesses of OoB and VLM detectors to domain shift. OoB detectors rely heavily on fingerprints and low-level arti-

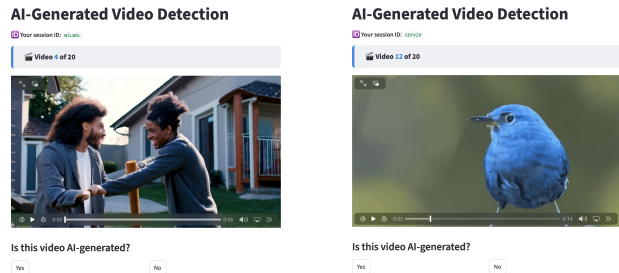


Figure 7. **GUI for user study:** Participants classify videos as real or fake, we show full-fake (left) and FakeParts (right) examples.

facts [8], which are inconsistent across modern generators, while VLMs depend strongly on their fine-tuning distribution and thus fail to generalize to synthetic, stylized, or partially edited content. FoM detectors, many of which are CLIP-based, leverage semantic-level representations, enabling good generalization across full-fake videos and some FakeParts. However, semantic or SSL-style features tend to overlook small, localized edits; real pixels can dilute forged regions. A clear example is *Face*, where edit areas are small and no FoM exceeds 60% AUC. By contrast, diffusion-based detectors achieve the best balance as their reconstruction-based mechanism evaluates whether inputs lie on the manifold of real data, rather than depending on semantic cues or brittle low-level fingerprints [16, 68, 128]. This allows them to capture subtle artifacts in both full-fake and FakeParts, resulting in uniformly strong performances.

5.2. Human Perception Study

To assess human detection capabilities, we conducted a user study using a Streamlit-based survey. A total of 290 participants each labelled 20 randomly selected video clips (real or FakeParts), yielding approximately 5800 annotations overall, half corresponding to real content and half to videos containing *FakeParts*. Humans achieved an average of 77.3% accuracy, outperforming most automated methods, especially on partial fakes *Interpolation*, *Extrapolation*, *Inpainting*, *Outpainting*, *Faceswap* and *Style Change*.

6. Conclusion

We introduced **FakePartsBench**, the first benchmark for detecting *FakeParts*, deepfakes with localized manipulations in otherwise authentic videos. These subtle edits exploit real context, severely reducing the performance of both human annotators and state-of-the-art detectors. By providing fine-grained spatial and temporal annotations, FakePartsBench enables rigorous evaluation under partial manipulations. We hope it drives progress toward detectors that capture fine-grained inconsistencies and uphold media integrity against evolving generative manipulations.

Limitations. While we cover diverse manipulation types, finer-grained exploration, such as varying inpainting areas and their effect on detection, remains open. Moreover, although our goal is to strengthen detection, we recognize potential risks of misuse; our focus remains strictly on defense and mitigation for trustworthy AI.

Acknowledgements

This work is supported by Hi!PARIS and ANR/France 2030 program (ANR-23-IACL-0005) and ANR APATE (ANR-22-CE39-0016), CIEDS vague 4, Hi!Paris grant, postdoctoral fellowship and Professor Monge chair.

This project was granted access to the IDRIS High-Performance Computing (HPC) resources under the allocation 20XX-AD011015141R2 made by GENCI (Grand Équipement National de Calcul Intensif). We sincerely thank Eleftherios Tsonis for his meticulous proofreading.

References

- [1] Shruti Agarwal, Tarek El-Gaaly, Hany Farid, and Ser-Nam Lim. Detecting deep-fake videos from phoneme-viseme mismatches. *Frontiers in Artificial Intelligence*, 3(59), 2020. 2, 3
- [2] Arslan Ali, Junjie Bai, Maciej Bala, Yogesh Balaji, Aaron Blakeman, Tiffany Cai, Jiaxin Cao, Tianshi Cao, Elizabeth Cha, Yu-Wei Chao, et al. Cosmos-predict2: General-purpose world foundation models for physical ai. <https://github.com/nvidia-cosmos/cosmos-predict2>, 2025. GitHub repository, Apache-2.0 license. 5, 6, 16, 19, 20
- [3] Xiang An, Xuhan Zhu, Yuan Gao, Yang Xiao, Yongle Zhao, Ziyong Feng, Lan Wu, Bin Qin, Ming Zhang, Debing Zhang, and Ying Fu. Partial fc: Training 10 million identities on a single machine. In *Int. Conf. Comput. Vis. Worksh.*, 2021. 5, 18
- [4] Xiang An, Jiangkang Deng, Jia Guo, Ziyong Feng, Xuhan Zhu, Yang Jing, and Liu Tongliang. Killing two birds with one stone: Efficient and robust training of face recognition cnns by partial fc. In *IEEE Conf. Comput. Vis. Pattern Recognit.*, 2022. 5, 18
- [5] Titas Anciukevičius, Zexiang Xu, Matthew Fisher, Paul Henderson, Hakan Bilen, Niloy J Mitra, and Paul Guerrero. Renderdiffusion: Image diffusion for 3d reconstruction, inpainting and generation. In *IEEE Conf. Comput. Vis. Pattern Recognit.*, pages 12608–12618, 2023. 20
- [6] Jianfa Bai, Man Lin, Gang Cao, and Zijie Lou. Ai-generated video detection via spatial-temporal anomaly learning. In *Chinese Conference on Pattern Recognition and Computer Vision (PRCV)*. Springer, 2024. 3, 6, 7
- [7] Max Bain, Arsha Nagrani, Gül Varol, and Andrew Zisserman. Frozen in time: A joint video and image encoder for end-to-end retrieval. In *Int. Conf. Comput. Vis.*, 2021. 3
- [8] Quentin Bammey. Synthbuster: Towards detection of diffusion model generated images. *IEEE Open Journal of Signal Processing*, 5:1–9, 2023. 8
- [9] Quentin Bammey. Synthbuster: Towards detection of diffusion model generated images. *IEEE Open Journal of Signal Processing*, 5:1–9, 2024. 2
- [10] Andreas Blattmann, Tim Dockhorn, Sumith Kulal, Daniel Mendeleevitch, Maciej Kilian, Dominik Lorenz, Yam Levi, Zion English, Vikram Voleti, Adam Letts, et al. Stable video diffusion: Scaling latent video diffusion models to large datasets. *arXiv preprint arXiv:2311.15127*, 2023. 3, 5, 20
- [11] Andrew Brock, Jeff Donahue, and Karen Simonyan. Large scale gan training for high fidelity natural image synthesis. *arXiv preprint arXiv:1809.11096*, 2018. 2
- [12] Tim Brooks, Bill Peebles, Connor Holmes, Will DePue, and Yufei Guo. Video generation models as world simulators. <https://openai.com/research/video-generation-models-as-world-simulators>, 2024. Accessed: 2025-05-07. 2, 3, 4, 5, 16, 17, 19, 21
- [13] Zhixi Cai, Shreya Ghosh, Aman Pankaj Adatia, Munawar Hayat, Abhinav Dhall, Tom Gedeon, and Kalin Stefanov. Av-deepfake1m: A large-scale llm-driven audio-visual deepfake dataset. In *ACM Int. Conf. Multimedia*, 2024. 3
- [14] Saurabh Chandra, Johanna Murtfeldt, Zihang Qiu, Anirban Karmakar, Ming-Hsuan Lee, Joshua Tanumihardja, Basma Farhat, Steven Caffee, Junghyun Paik, Kyoung Mu Lee, et al. Deepfakebench: A unified benchmark for deepfake detection. In *IEEE Conf. Comput. Vis. Pattern Recognit.*, 2024. 2
- [15] You-Ming Chang, Chen Yeh, Wei-Chen Chiu, and Ning Yu. Antifakeprompt: Prompt-tuned vision-language models are fake image detectors. *arXiv preprint arXiv:2310.17419*, 2023. 6, 7
- [16] Baoying Chen, Jishen Zeng, Jianquan Yang, and Rui Yang. DRCT: Diffusion reconstruction contrastive training towards universal detection of diffusion generated images. In *Proceedings of the 41st International Conference on Machine Learning*, pages 7621–7639. PMLR, 2024. 6, 7, 8, 15, 17, 18
- [17] Haoxing Chen, Yan Hong, Zizheng Huang, Zhuoer Xu, Zhangxuan Gu, Yaohui Li, Jun Lan, Huijia Zhu, Jianfu Zhang, Weiqiang Wang, et al. Demamba: Ai-generated video detection on million-scale genvideo benchmark. *arXiv preprint arXiv:2405.19707*, 2024. 3
- [18] Haoxin Chen, Yong Zhang, Xiaodong Cun, Menghan Xia, Xintao Wang, Chao Weng, and Ying Shan. Videocrafter2:

- Overcoming data limitations for high-quality video diffusion models. In *IEEE Conf. Comput. Vis. Pattern Recognit.*, 2024. 2, 3
- [19] Yu Chen, Weilin Sun, Xiaoqian Zhou, Tao Lin, Peng Sun, Jun Cao, and Rongrong Ji. Ummaformer: Unified multi-modal manipulation detection transformer. In *IEEE Conf. Comput. Vis. Pattern Recognit.*, 2024. 2
- [20] Yunzhuo Chen, Naveed Akhtar, Nur Al Hasan Haldar, and Ajmal Mian. Deepfake detection with spatio-temporal consistency and attention. *arXiv preprint arXiv:2502.08216*, 2025. 2
- [21] Vincent Christlein, Christian Riess, Johannes Jordan, Corinna Riess, and Elli Angelopoulou. An evaluation of popular copy-move forgery detection approaches. *IEEE Transactions on Information Forensics and Security*, 7(6): 1841–1854, 2012. 2
- [22] Beilin Chu, Xuan Xu, Weike You, and Linna Zhou. Unearthing common inconsistency for generalisable deepfake detection. *arXiv preprint arXiv:2311.11549*, 2023. 2
- [23] Google Cloud. Veo2, 2025. Accessed: 2025-05-07. 3, 4, 5, 16, 17, 19, 21
- [24] Riccardo Corvi, Davide Cozzolino, Giovanni Poggi, Koki Nagano, and Luisa Verdoliva. Intriguing properties of synthetic images: From generative adversarial networks to diffusion models. In *IEEE Conf. Comput. Vis. Pattern Recognit. Worksh.*, 2023. 2
- [25] Riccardo Corvi, Davide Cozzolino, Giada Zingarini, Giovanni Poggi, Koki Nagano, and Luisa Verdoliva. On the detection of synthetic images generated by diffusion models. In *IEEE International Conference on Acoustics, Speech and Signal Processing (ICASSP)*, pages 1–5. IEEE, 2023. 2
- [26] Davide Cozzolino, Andreas Rössler, Justus Thies, Matthias Nießner, and Luisa Verdoliva. Id-reveal: Identity-aware deepfake video detection. In *ICCV*, page 15088–15097, 2021. 2
- [27] Davide Cozzolino, Giovanni Poggi, Riccardo Corvi, Matthias Nießner, and Luisa Verdoliva. Raising the bar of ai-generated image detection with clip. In *IEEE Conf. Comput. Vis. Pattern Recognit. Worksh.*, pages 4356–4366, 2024. 2
- [28] Jiankang Deng, Anastasios Roussos, Grigorios Chrysos, Evangelos Ververas, Irene Kotsia, Jie Shen, and Stefanos Zafeiriou. The menpo benchmark for multi-pose 2d and 3d facial landmark localisation and tracking. *Int. J. Comput. Vis.*, 2018. 5, 18
- [29] Jiankang Deng, Jia Guo, Xue Niannan, and Stefanos Zafeiriou. Arcface: Additive angular margin loss for deep face recognition. In *IEEE Conf. Comput. Vis. Pattern Recognit.*, 2019. 5, 16, 19
- [30] Jiankang Deng, Jia Guo, Tongliang Liu, Mingming Gong, and Stefanos Zafeiriou. Sub-center arcface: Boosting face recognition by large-scale noisy web faces. In *Eur. Conf. Comput. Vis.*, 2020.
- [31] Jiankang Deng, Jia Guo, Evangelos Ververas, Irene Kotsia, and Stefanos Zafeiriou. Retinaface: Single-shot multi-level face localisation in the wild. In *IEEE Conf. Comput. Vis. Pattern Recognit.*, 2020. 5, 18
- [32] Henghui Ding, Chang Liu, Shuting He, Xudong Jiang, Philip HS Torr, and Song Bai. MOSE: A new dataset for video object segmentation in complex scenes. In *Int. Conf. Comput. Vis.*, 2023. 4
- [33] Brian Dolhansky, Joanna Bitton, Ben Pflaum, Jikuo Lu, Russ Howes, Menglin Wang, and Cristian Canton Ferrer. The deepfake detection challenge (dfdc) dataset. *arXiv preprint arXiv:2006.07397*, 2020. 2, 3
- [34] NVIDIA Team et al. Cosmos world foundation model platform for physical ai, 2025. 5, 6, 16, 20
- [35] NVIDIA Team et al. World simulation with video foundation models for physical ai, 2025. 6
- [36] Hany Farid. Image forgery detection. *IEEE Signal Processing Magazine*, 26(2):16–25, 2009. 2
- [37] Runze Feng, Jiahao Chen, and Andrew Owens. Understanding the detection of deepfake videos through temporal attention. *IEEE Transactions on Image Processing*, 32(4): 2450–2462, 2023. 2
- [38] Songwei Ge, Aniruddha Mahapatra, Gaurav Parmar, Jun-Yan Zhu, and Jia-Bin Huang. On the content bias in fréchet video distance. In *IEEE Conf. Comput. Vis. Pattern Recognit.*, pages 7277–7288, 2024. 3
- [39] Baris Gecer, Jiankang Deng, and Stefanos Zafeiriou. Ostec: One-shot texture completion. In *IEEE Conf. Comput. Vis. Pattern Recognit.*, 2021. 5, 18
- [40] Ian Goodfellow, Jean Pouget-Abadie, Mehdi Mirza, Bing Xu, David Warde-Farley, Sherjil Ozair, Aaron Courville, and Yoshua Bengio. Generative adversarial networks. *Communications of the ACM*, 63(11):139–144, 2020. 2
- [41] D. Gragnaniello, D. Cozzolino, F. Marra, G. Poggi, and L. Verdoliva. Are gan generated images easy to detect? a critical analysis of the state-of-the-art. In *2021 IEEE International Conference on Multimedia and Expo (ICME)*, pages 1–6, 2021. 2
- [42] Albert Gu and Tri Dao. Mamba: Linear-time sequence modeling with selective state spaces. *arXiv preprint arXiv:2312.00752*, 2023. 3
- [43] Luca Guarnera, Oliver Giudice, and Sebastiano Battiato. Deepfake detection by analyzing convolutional traces. In *IEEE Conf. Comput. Vis. Pattern Recognit. Worksh.*, pages 666–667, 2020. 2
- [44] Jia Guo, Jiankang Deng, Niannan Xue, and Stefanos Zafeiriou. Stacked dense u-nets with dual transformers for robust face alignment. In *Brit. Mach. Vis. Conf.*, 2018. 5, 18
- [45] Jia Guo, Jiankang Deng, Alexandros Lattas, and Stefanos Zafeiriou. Sample and computation redistribution for efficient face detection. *arXiv preprint arXiv:2105.04714*, 2021. 5, 18
- [46] Xiao Guo, Xiaohong Liu, Zhiyuan Ren, Steven Grosz, Iacopo Masi, and Xiaoming Liu. Hierarchical fine-grained image forgery detection and localization. In *CVPR*, 2023. 6, 7
- [47] Yuwei Guo, Ceyuan Yang, Anyi Rao, Zhengyang Liang, Yaohui Wang, Yu Qiao, Maneesh Agrawala, Dahua Lin, and Bo Dai. Animatediff: Animate your personalized text-to-image diffusion models without specific tuning. In *Int. Conf. Learn. Represent.*, 2023. 2, 3

- [48] David Güera and Edward J. Delp. Deepfake video detection using recurrent neural networks. In *2018 15th IEEE International Conference on Advanced Video and Signal Based Surveillance (AVSS)*, page 1–6, 2018. 2, 3
- [49] Yoav HaCohen, Nisan Chiprut, Benny Brazowski, Daniel Shalem, Dudu Moshe, Eitan Richardson, Eran Levin, Guy Shiran, Nir Zabari, Ori Gordon, Poriya Panet, Sapir Weissbuch, Victor Kulikov, Yaki Bitterman, Zeev Melumian, and Ofir Bibi. Ltx-video: Realtime video latent diffusion, 2024. 4, 5, 16, 17, 19
- [50] Alexandros Haliassos, Konstantinos Vougioukas, Stavros Petridis, and Maja Pantic. Lips don't lie: A generalisable and robust approach to face forgery detection. In *IEEE Conf. Comput. Vis. Pattern Recognit.*, pages 5039–5049, 2021. 3
- [51] Hao He, Yinghao Xu, Yuwei Guo, Gordon Wetzstein, Bo Dai, Hongsheng Li, and Ceyuan Yang. Cameractrl: Enabling camera control for text-to-video generation. *arXiv preprint arXiv:2404.02101*, 2024. 2, 3, 5, 20
- [52] Yinan He, Bei Gan, Siyu Chen, Yichun Zhou, Guojun Yin, Luchuan Song, Lu Sheng, Jing Shao, and Ziwei Liu. Forgerynet: A versatile benchmark for comprehensive forgery analysis. In *IEEE Conf. Comput. Vis. Pattern Recognit.*, pages 4360–4369, 2021. 3
- [53] Chih-Chung Hsu, Tzu-Yi Hung, Chia-Wen Lin, and Chiou-Ting Hsu. Video forgery detection using correlation of noise residue. In *2008 IEEE 10th workshop on multimedia signal processing*, pages 170–174. IEEE, 2008. 2
- [54] Yihao Huang, Felix Juefei-Xu, Qing Guo, Yang Liu, and Geguang Pu. Fakelocator: Robust localization of gan-based face manipulations. *IEEE Transactions on Information Forensics and Security*, 17:2657–2672, 2022. 2
- [55] Ziqi Huang, Yinan He, Jiashuo Yu, Fan Zhang, Chenyang Si, Yuming Jiang, Yuanhan Zhang, Tianxing Wu, Qingyang Jin, Nattapol Chanpaisit, et al. Vbench: Comprehensive benchmark suite for video generative models. In *IEEE Conf. Comput. Vis. Pattern Recognit.*, pages 21807–21818, 2024. 4
- [56] Zhenglin Huang, Jinwei Hu, Xiangtai Li, Yiwei He, Xingyu Zhao, Bei Peng, Baoyuan Wu, Xiaowei Huang, and Guangliang Cheng. SIDA: social media image deepfake detection, localization and explanation with large multimodal model. In *IEEE Conf. Comput. Vis. Pattern Recognit.*, 2025. 6, 7, 15
- [57] Siddhant Jain, Daniel Watson, Eric Tabellion, Ben Poole, Janne Kontkanen, et al. Video interpolation with diffusion models. In *IEEE Conf. Comput. Vis. Pattern Recognit.*, pages 7341–7351, 2024. 2
- [58] Liming Jiang, Wayne Li, Ziqi Wu, Yujun Qian, and Chen Change Loy. Deeperforensics-1.0: A large-scale dataset for real-world face forgery detection. In *IEEE Conf. Comput. Vis. Pattern Recognit.*, 2020. 3
- [59] Ozgur Kara, Bariscan Kurtkaya, Hidir Yesiltepe, James M Rehg, and Pinar Yanardag. Rave: Randomized noise shuffling for fast and consistent video editing with diffusion models. In *IEEE Conf. Comput. Vis. Pattern Recognit.*, pages 6507–6516, 2024. 5, 6, 16, 19, 20
- [60] Johanna Karras, Aleksander Holynski, Ting-Chun Wang, and Ira Kemelmacher-Shlizerman. Dreampose: Fashion image-to-video synthesis via stable diffusion. In *Int. Conf. Comput. Vis.*, pages 22623–22633. IEEE, 2023. 3
- [61] Tero Karras, Samuli Laine, and Timo Aila. A style-based generator architecture for generative adversarial networks. In *IEEE Conf. Comput. Vis. Pattern Recognit.*, pages 4401–4410, 2019. 2, 3
- [62] Hasam Khalid, Shahroz Tariq, Minha Kim, and Simon S Woo. Fakeavceleb: A novel audio-video multimodal deepfake dataset. In *Adv. Neural Inf. Process. Syst.*, 2021. 3
- [63] Michihiro Kobayashi, Takahiro Okabe, and Yoichi Sato. Detecting forgery from static-scene video based on inconsistency in noise level functions. *IEEE Transactions on Information Forensics and Security*, 5(4):883–892, 2010. 2
- [64] Weijie Kong, Qi Tian, Zijian Zhang, Rox Min, Zuozhuo Dai, Jin Zhou, Jiangfeng Xiong, Xin Li, Bo Wu, Jianwei Zhang, et al. Hunyuanvideo: A systematic framework for large video generative models. *arXiv preprint arXiv:2412.03603*, 2024. 4, 5, 16, 17, 19
- [65] Pavel Korshunov, Haolin Chen, Philip N Garner, and Sébastien Marcel. Vulnerability of automatic identity recognition to audio-visual deepfakes. In *2023 IEEE International Joint Conference on Biometrics (IJCB)*, pages 1–10. IEEE, 2023. 3
- [66] Max Ku, Cong Wei, Weiming Ren, Harry Yang, and Wenhui Chen. Anyv2v: A tuning-free framework for any video-to-video editing tasks, 2024. 5, 6, 16, 19, 20
- [67] Patrick Kwon, Jaeseong You, Gyuhyeon Nam, Sungwoo Park, and Gyeongsu Chae. Kodf: A large-scale korean deepfake detection dataset. In *Int. Conf. Comput. Vis.*, pages 10744–10753, 2021. 2
- [68] Alexander C Li, Mihir Prabhudesai, Shivam Duggal, Ellis Brown, and Deepak Pathak. Your diffusion model is secretly a zero-shot classifier. In *IEEE Conf. Comput. Vis. Pattern Recognit.*, pages 2206–2217, 2023. 8
- [69] Lingzhi Li, Jianmin Bao, Ting Zhang, Hao Yang, Dong Chen, Fang Wen, and Baining Guo. Face x-ray for more general face forgery detection. In *IEEE Conf. Comput. Vis. Pattern Recognit.*, pages 5001–5010, 2020. 2
- [70] Xiaowen Li, Haolan Xue, Peiran Ren, and Liefeng Bo. Diffuseraser: A diffusion model for video inpainting. *arXiv preprint arXiv:2501.10018*, 2025. 5, 16, 19
- [71] Xinhao Li, Ziang Yan, Desen Meng, Lu Dong, Xiangyu Zeng, Yinan He, Yali Wang, Yu Qiao, Yi Wang, and Limin Wang. Videochat-r1: Enhancing spatio-temporal perception via reinforcement fine-tuning. *arXiv preprint arXiv:2504.06958*, 2025. 6, 20
- [72] Yuezun Li and Siwei Lyu. Exposing deepfake videos by detecting face warping artifacts. *arXiv preprint arXiv:1811.00656*, 2018. 2
- [73] Yuezun Li, Xin Yang, Pu Sun, Honggang Qi, and Siwei Lyu. Celeb-df: A large-scale challenging dataset for deepfake forensics. In *IEEE Conf. Comput. Vis. Pattern Recognit.*, pages 3207–3216, 2020. 5, 18
- [74] Zhen Li, Cheng-Ze Lu, Jianhua Qin, Chun-Le Guo, and Ming-Ming Cheng. Towards an end-to-end framework for

- flow-guided video inpainting. In *IEEE Conf. Comput. Vis. Pattern Recognit.*, pages 17562–17571, 2022. 5
- [75] Baoping Liu, Bo Liu, Ming Ding, Tianqing Zhu, and Xin Yu. Ti2net: Temporal identity inconsistency network for deepfake detection. In *Proceedings of the IEEE/CVF Winter Conference on Applications of Computer Vision (WACV)*, pages 4691–4700, 2023. 2
- [76] Honggu Liu, Xiaodan Li, Wenbo Zhou, Yuefeng Chen, Yuan He, Hui Xue, Weiming Zhang, and Nenghai Yu. Spatial-phase shallow learning: Rethinking face forgery detection in frequency domain. In *IEEE Conf. Comput. Vis. Pattern Recognit.*, pages 772–781, 2021. 2
- [77] Huan Liu, Zichang Tan, Chuangchuang Tan, Yunchao Wei, Jingdong Wang, and Yao Zhao. Forgery-aware adaptive transformer for generalizable synthetic image detection. In *IEEE Conf. Comput. Vis. Pattern Recognit.*, 2024. 6, 7
- [78] Jiaxin Liu, Jia Wang, Saihui Hou, Min Ren, Huijia Wu, Long Ma, Renwang Pei, and Zhaofeng He. Beyond face swapping: A diffusion-based digital human benchmark for multimodal deepfake detection. *arXiv preprint arXiv:2505.16512*, 2025. 3
- [79] Ziwei Liu, Ping Luo, Xiaogang Wang, and Xiaoou Tang. Deep learning face attributes in the wild. In *Int. Conf. Comput. Vis.*, 2015. 5, 18
- [80] Andreas Lugmayr, Martin Danelljan, Andres Romero, Fisher Yu, Radu Timofte, and Luc Van Gool. Repaint: Inpainting using denoising diffusion probabilistic models. In *IEEE Conf. Comput. Vis. Pattern Recognit.*, pages 11461–11471, 2022. 20
- [81] Long Ma, Zhiyuan Yan, Qinglang Guo, Yong Liao, Haiyang Yu, and Pengyuan Zhou. Detecting ai-generated video via frame consistency. *arXiv preprint arXiv:2402.02085*, 2024. 3
- [82] Ruipeng Ma, Jinhao Duan, Fei Kong, Xiaoshuang Shi, and Kaidi Xu. Exposing the fake: Effective diffusion-generated images detection. *arXiv preprint arXiv:2307.06272*, 2023. 2
- [83] Xiaochen Ma, Bo Du, Zhuohang Jiang, Ahmed Y Al Hammadi, and Jizhe Zhou. Iml-vit: Benchmarking image manipulation localization by vision transformer. *arXiv preprint arXiv:2307.14863*, 2023. 6, 7
- [84] Francesco Marra, Diego Gagnaniello, Davide Cozzolino, and Luisa Verdoliva. Detection of gan-generated fake images over social networks. In *2018 IEEE Conference on Multimedia Information Processing and Retrieval (MIPR)*, pages 384–389, 2018. 2
- [85] Iacopo Masi, Aditya Killekar, Royston Marian Mascarenhas, Shenoy Pratik Gurudatt, and Wael AbdAlmageed. Two-branch recurrent network for isolating deepfakes in videos. In *Eur. Conf. Comput. Vis.*, pages 667–684. Springer, 2020. 2, 3
- [86] Corran McCallum. pexelvideos. <https://huggingface.co/datasets/Corran/pexelvideos>, 2022. Accessed: 2025-08-01. 4, 17
- [87] Xun Long Ng, Kian Eng Ong, Qichen Zheng, Yun Ni, Si Yong Yeo, and Jun Liu. Animal kingdom: A large and diverse dataset for animal behavior understanding. In *IEEE Conf. Comput. Vis. Pattern Recognit.*, pages 19023–19034, 2022. 6, 20
- [88] Zhenliang Ni, Qiangyu Yan, Mouxiao Huang, Tianning Yuan, Yehui Tang, Hailin Hu, Xinghao Chen, and Yunhe Wang. Genvidbench: A challenging benchmark for detecting ai-generated video. *arXiv preprint arXiv:2501.11340*, 2025. 3
- [89] Yuval Nirkin, Yosi Keller, and Tal Hassner. Fsgan: Subject agnostic face swapping and reenactment. In *Int. Conf. Comput. Vis.*, pages 7184–7193, 2019. 2, 3
- [90] Utkarsh Ojha, Yuheng Li, and Yong Jae Lee. Towards universal fake image detectors that generalize across generative models. In *IEEE Conf. Comput. Vis. Pattern Recognit.*, pages 24480–24489, 2023. 2, 6, 7
- [91] F. Perazzi, J. Pont-Tuset, B. McWilliams, L. Van Gool, M. Gross, and A. Sorkine-Hornung. A benchmark dataset and evaluation methodology for video object segmentation. In *IEEE Conf. Comput. Vis. Pattern Recognit.*, 2016. 4
- [92] Ivan Perov, Daiheng Gao, Nikolay Chervoniy, Kunlin Liu, Sugasa Marangonda, Chris Umé, Carl Shift Facenheim, Luis RP, Jian Jiang, Sheng Zhang, et al. Deepfacelab: Integrated, flexible and extensible face-swapping framework. *arXiv preprint arXiv:2005.05535*, 2020. 2, 3
- [93] Jordi Pont-Tuset, Federico Perazzi, Sergi Caelles, Pablo Arbeláez, Alex Sorkine-Hornung, and Luc Van Gool. The 2017 davis challenge on video object segmentation. *arXiv preprint arXiv:1704.00675*, 2017. 4
- [94] Yuyang Qian, Guojun Yin, Lu Sheng, Zixuan Chen, and Jing Shao. Thinking in frequency: Face forgery detection by mining frequency-aware clues. In *Eur. Conf. Comput. Vis.*, pages 86–103. Springer, 2020. 2
- [95] Yuyang Qian, Guojun Yin, Lu Sheng, Zixuan Chen, and Jing Shao. Thinking in frequency: Face forgery detection by mining frequency-aware clues. In *Eur. Conf. Comput. Vis.*, pages 86–103. Springer, 2020. 2
- [96] Alec Radford, Jong Wook Kim, Chris Hallacy, Aditya Ramesh, Gabriel Goh, Sandhini Agarwal, Girish Sastry, Amanda Askell, Pamela Mishkin, Jack Clark, et al. Learning transferable visual models from natural language supervision. In *Int. Conf. Mach. Learn.*, pages 8748–8763. PmlR, 2021. 2, 6
- [97] Nikhila Ravi, Valentin Gabeur, Yuan-Ting Hu, Ronghang Hu, Chaitanya Ryali, Tengyu Ma, Haitham Khedr, Roman Rädle, Chloe Rolland, Laura Gustafson, et al. Sam 2: Segment anything in images and videos. *arXiv preprint arXiv:2408.00714*, 2024. 5, 19
- [98] Fitsum Reda, Janne Kontkanen, Eric Tabellion, Deqing Sun, Caroline Pantofaru, and Brian Curless. Film: Frame interpolation for large motion. In *Eur. Conf. Comput. Vis.*, pages 250–266. Springer, 2022. 3
- [99] Xingyu Ren, Alexandros Lattas, Baris Gecer, Jiankang Deng, Chao Ma, and Xiaokang Yang. Facial geometric detail recovery via implicit representation. In *International Conference on Automatic Face and Gesture Recognition (FG)*, 2023. 5, 18
- [100] Jonas Ricker, Simon Damm, Thorsten Holz, and Asja Fischer. Towards the detection of diffusion model deepfakes.

- Proceedings of the 37th AAAI Conference on Artificial Intelligence*, 37:446–457, 2023. 2
- [101] Andreas Rossler, Davide Cozzolino, Luisa Verdoliva, Christian Riess, Justus Thies, and Matthias Nießner. Face-forensics++: Learning to detect manipulated facial images. In *Int. Conf. Comput. Vis.*, pages 1–11, 2019. 2, 3
- [102] Ekraam Sabir, Jing Cheng, Ajinkya Jaiswal, Wael AbdAlmageed, Iacopo Masi, and Prem Natarajan. Recurrent convolutional strategies for face manipulation detection in videos. In *IEEE Conf. Comput. Vis. Pattern Recognit. Worksh.*, 2019. 2
- [103] Zeyang Sha, Zheng Li, Ning Yu, and Yang Zhang. De-fake: Detection and attribution of fake images generated by text-to-image generation models. In *Proceedings of the 2023 ACM SIGSAC conference on computer and communications security*, pages 3418–3432, 2023. 6, 7
- [104] Rui Shao, Tianxing Wu, and Ziwei Liu. Detecting and recovering sequential deepfake manipulation. In *Eur. Conf. Comput. Vis.*, pages 712–728. Springer, 2022. 2
- [105] Rui Shao, Tianxing Wu, and Ziwei Liu. Detecting and grounding multi-modal media manipulation. In *IEEE Conf. Comput. Vis. Pattern Recognit.*, pages 6904–6913, 2023. 2
- [106] Yujun Shen, Jinjin Gu, Xiaou Tang, and Bolei Zhou. Interpreting the latent space of gans for semantic face editing. In *IEEE Conf. Comput. Vis. Pattern Recognit.*, 2020. 2, 3
- [107] Kaede Shiohara and Toshihiko Yamasaki. Detecting deepfakes with self-blended images. In *IEEE Conf. Comput. Vis. Pattern Recognit.*, 2022. 2
- [108] Xiufeng Song, Xiao Guo, Jiache Zhang, Qirui Li, Lei Bai, Xiaoming Liu, Guangtao Zhai, and Xiaohong Liu. On learning multi-modal forgery representation for diffusion generated video detection. In *Adv. Neural Inf. Process. Syst.*, 2024. 6, 7
- [109] Xiufeng Song, Xiao Guo, Jiache Zhang, Qirui Li, Lei Bai, Xiaoming Liu, Guangtao Zhai, and Xiaohong Liu. On learning multi-modal forgery representation for diffusion generated video detection. *arXiv preprint arXiv:2410.23623*, 2024. 3
- [110] Andreas Steiner, André Susano Pinto, Michael Tschannen, Daniel Keysers, Xiao Wang, Yonatan Bitton, Alexey Gritsenko, Matthias Minderer, Anthony Sherbondy, Shangbang Long, et al. Paligemma 2: A family of versatile vlms for transfer. *arXiv preprint arXiv:2412.03555*, 2024. 4, 6, 20
- [111] Chuangchuang Tan, Yao Zhao, Shikui Wei, Guanghua Gu, and Yunchao Wei. Learning on gradients: Generalized artifacts representation for gan-generated images detection. In *IEEE Conf. Comput. Vis. Pattern Recognit.*, pages 12105–12114, 2023. 2
- [112] Chuangchuang Tan, Yao Zhao, Shikui Wei, Guanghua Gu, Ping Liu, and Yunchao Wei. Rethinking the up-sampling operations in cnn-based generative network for generalizable deepfake detection. In *IEEE Conf. Comput. Vis. Pattern Recognit.*, pages 28130–28139, 2024. 6, 7
- [113] Chuangchuang Tan, Renshuai Tao, Huan Liu, Guanghua Gu, Baoyuan Wu, Yao Zhao, and Yunchao Wei. C2p-clip: Injecting category common prompt in clip to enhance generalization in deepfake detection. In *AAAI Conf. Artif. Intell.*, 2025. 6, 7, 15
- [114] Shahroz Tariq, Sangyup Lee, and Simon Woo. One detector to rule them all: Towards a general deepfake attack detection framework. In *Proceedings of the Web Conference 2021*, page 3625–3637, New York, NY, USA, 2021. Association for Computing Machinery. 2
- [115] Genmo Team. Mochi 1. <https://github.com/genmoai/models>, 2024. 4, 5, 16, 17, 19
- [116] Gemini Team, Rohan Anil, Sebastian Borgeaud, Jean-Baptiste Alayrac, Jiahui Yu, Radu Soricut, Johan Schalkwyk, Andrew M Dai, Anja Hauth, Katie Millican, et al. Gemini: a family of highly capable multimodal models. *arXiv preprint arXiv:2312.11805*, 2023. 4, 17
- [117] Ayush Tewari, Mohamed Elgharib, Gaurav Bharaj, Florian Bernard, Hans-Peter Seidel, Patrick Perez, Michael Zollhofer, and Christian Theobalt. Stylerig: Rigging stylegan for 3d control over portrait images. In *IEEE Conf. Comput. Vis. Pattern Recognit.*, 2020. 2, 3
- [118] Justus Thies, Michael Zollhofer, Marc Stamminger, Christian Theobalt, and Matthias Niessner. Face2face: Real-time face capture and reenactment of rgb videos. In *IEEE Conf. Comput. Vis. Pattern Recognit.*, 2016.
- [119] Yu Tian, Xi Peng, Long Zhao, Shaoting Zhang, and Dimitris N Metaxas. Cr-gan: learning complete representations for multi-view generation. *arXiv preprint arXiv:1806.11191*, 2018. 2, 3
- [120] Team Wan, Ang Wang, Baole Ai, Bin Wen, Chaojie Mao, Chen-Wei Xie, Di Chen, Feiwu Yu, Haiming Zhao, Jianxiao Yang, et al. Wan: Open and advanced large-scale video generative models. *arXiv preprint arXiv:2503.20314*, 2025. 4, 5, 16, 17, 19
- [121] Junke Wang, Zuxuan Wu, Wenhao Ouyang, Xintong Han, Jingjing Chen, Ser-Nam Lim, and Yu-Gang Jiang. M2tr: Multi-modal multi-scale transformers for deepfake detection. In *Proceedings of the 2022 International Conference on Multimedia Retrieval (ICMR)*, pages 615–623. ACM, 2022. 2
- [122] Jiuniu Wang, Hangjie Yuan, Dayou Chen, Yingya Zhang, Xiang Wang, and Shiwei Zhang. Modelscope text-to-video technical report. *arXiv preprint arXiv:2308.06571*, 2023. 2
- [123] Sheng-Yu Wang, Oliver Wang, Richard Zhang, Andrew Owens, and Alexei A. Efros. Cnn-generated images are surprisingly easy to spot... for now. In *IEEE Conf. Comput. Vis. Pattern Recognit.*, 2020. 2
- [124] Sheng-Yu Wang, Oliver Wang, Richard Zhang, Andrew Owens, and Alexei A Efros. Cnn-generated images are surprisingly easy to spot... for now. In *IEEE Conf. Comput. Vis. Pattern Recognit.*, pages 8695–8704, 2020. 6, 7
- [125] Weihong Wang and Hany Farid. Exposing digital forgeries in video by detecting double mpeg compression. In *Proceedings of the 8th workshop on Multimedia and security*, pages 37–47, 2006. 2
- [126] Wenhao Wang and Yi Yang. Vidprom: A million-scale real prompt-gallery dataset for text-to-video diffusion models. In *Adv. Neural Inf. Process. Syst.*, 2024. 3, 4
- [127] Wen Wang, Qiuyu Wang, Kecheng Zheng, Hao Ouyang, Zhekai Chen, Biao Gong, Hao Chen, Yujun Shen, and Chunhua Shen. Framer: Interactive frame interpolation.

- arXiv preprint arXiv:2410.18978*, 2024. [2](#), [3](#), [5](#), [6](#), [16](#), [19](#), [20](#)
- [128] Xi Wang and Vicky Kalogeiton. Your diffusion model is an implicit synthetic image detector. In *Eur. Conf. Comput. Vis. Worksh.*, 2024. [2](#), [8](#)
- [129] Xiaojuan Wang, Boyang Zhou, Brian Curless, Ira Kemelmacher-Shlizerman, Aleksander Holynski, and Steven M Seitz. Generative inbetweening: Adapting image-to-video models for keyframe interpolation. *arXiv preprint arXiv:2408.15239*, 2024. [2](#)
- [130] Xi Wang, Robin Courant, Marc Christie, and Vicky Kalogeiton. Akira: Augmentation kit on rays for optical video generation. In *IEEE Conf. Comput. Vis. Pattern Recognit.*, pages 2609–2619, 2025. [2](#), [3](#), [5](#), [16](#), [19](#), [20](#)
- [131] Yuan Wang, Kun Yu, Chen Chen, Xiyuan Hu, and Silong Peng. Dynamic graph learning with content-guided spatial-frequency relation reasoning for deepfake detection. In *IEEE Conf. Comput. Vis. Pattern Recognit.*, page 7278–7287, 2023. [2](#)
- [132] Zhendong Wang, Jianmin Bao, Wengang Zhou, Weilun Wang, and Houqiang Li. Altfreezing for more general video face forgery detection. In *IEEE Conf. Comput. Vis. Pattern Recognit.*, pages 4129–4138, 2023. [2](#)
- [133] Zhizhong Wang, Lei Zhao, and Wei Xing. Stylediffusion: Controllable disentangled style transfer via diffusion models. In *IEEE Conf. Comput. Vis. Pattern Recognit.*, pages 7677–7689, 2023. [3](#)
- [134] Zhouxia Wang, Ziyang Yuan, Xintao Wang, Yaowei Li, Tianshui Chen, Menghan Xia, Ping Luo, and Ying Shan. Motionctrl: A unified and flexible motion controller for video generation. In *ACM Trans. Graph.*, 2024. [2](#), [5](#), [20](#)
- [135] Siwei Wen, Junyan Ye, Peilin Feng, Hengrui Kang, Zichen Wen, Yize Chen, Jiang Wu, Wenjun Wu, Conghui He, and Weijia Li. Spot the fake: Large multimodal model-based synthetic image detection with artifact explanation. *arXiv preprint arXiv:2503.14905*, 2025. [6](#), [7](#)
- [136] Jianzong Wu, Xiangtai Li, Chenyang Si, Shangchen Zhou, Jingkang Yang, Jiangning Zhang, Yining Li, Kai Chen, Yunhai Tong, Ziwei Liu, et al. Towards language-driven video inpainting via multimodal large language models. In *IEEE Conf. Comput. Vis. Pattern Recognit.*, pages 12501–12511, 2024. [5](#), [16](#), [19](#), [20](#)
- [137] Wayne Wu, Yunxuan Zhang, Cheng Li, Chen Qian, and Chen Change Loy. Reenactgan: Learning to reenact faces via boundary transfer. In *Eur. Conf. Comput. Vis.*, 2018. [2](#), [3](#)
- [138] Tianwei Xiong, Yuqing Wang, Daquan Zhou, Zhijie Lin, Jiashi Feng, and Xihui Liu. Lvd-2m: A long-take video dataset with temporally dense captions. *arXiv preprint arXiv:2410.10816*, 2024. [4](#)
- [139] Dejie Xu, Weili Nie, Chao Liu, Sifei Liu, Jan Kautz, Zhangyang Wang, and Arash Vahdat. Camco: Camera-controllable 3d-consistent image-to-video generation. *arXiv preprint arXiv:2406.02509*, 2024. [5](#), [20](#)
- [140] Yuting Xu, Jian Liang, Gengyun Jia, Ziming Yang, Yanhao Zhang, and Ran He. Tall: Thumbnail layout for deepfake video detection. In *IEEE Conf. Comput. Vis. Pattern Recognit.*, pages 22658–22668, 2023. [2](#)
- [141] Zhiyuan Yan, Taiping Yao, Shen Chen, Yandan Zhao, Xinghe Fu, Junwei Zhu, Donghao Luo, Chengjie Wang, Shouhong Ding, Yunsheng Wu, and Li Yuan. Df40: Toward next-generation deepfake detection. In *IEEE Conf. Comput. Vis. Pattern Recognit.*, 2024. [3](#)
- [142] Linjie Yang, Yuchen Fan, and Ning Xu. The 2nd large-scale video object segmentation challenge - video object segmentation track. In *Int. Conf. Comput. Vis.*, 2019. [4](#), [20](#)
- [143] Yongqi Yang, Zhihao Qian, Ye Zhu, Olga Russakovsky, and Yu Wu. D3: Scaling up deepfake detection by learning from discrepancy. In *IEEE Conf. Comput. Vis. Pattern Recognit.*, 2025. [6](#), [7](#), [15](#)
- [144] Zhuoyi Yang, Jiayan Teng, Wendi Zheng, Ming Ding, Shiyu Huang, Jiazheng Xu, Yuanming Yang, Wenyi Hong, Xiaohan Zhang, Guanyu Feng, et al. Cogvideox: Text-to-video diffusion models with an expert transformer. *arXiv preprint arXiv:2408.06072*, 2024. [4](#), [5](#), [16](#), [17](#), [19](#)
- [145] Ning Yu, Larry S. Davis, and Mario Fritz. Attributing fake images to gans: Learning and analyzing gan fingerprints. In *Int. Conf. Comput. Vis.*, 2019. [2](#)
- [146] DaiChi Zhang, Fanzhao Lin, Yingying Hua, Pengju Wang, Dan Zeng, and Shiming Ge. Deepfake video detection with spatiotemporal dropout transformer. In *Proceedings of the 30th ACM International Conference on Multimedia*, page 5833–5841, Lisboa Portugal, 2022. ACM. [2](#)
- [147] Rui Zhang, Hongxia Wang, Mingshan Du, Hanqing Liu, Yang Zhou, and Qiang Zeng. Ummaformer: A universal multimodal-adaptive transformer framework for temporal forgery localization. In *ACM Int. Conf. Multimedia*, pages 8749–8759, 2023. [3](#)
- [148] Xu Zhang, Svebor Karaman, and Shih-Fu Chang. Detecting and simulating artifacts in gan fake images. In *2019 IEEE International Workshop on Information Forensics and Security (WIFS)*, pages 1–6, 2019. [2](#)
- [149] Yue Zhang, Ben Colman, Xiao Guo, Ali Shahriyari, and Gaurav Bharaj. Common sense reasoning for deepfake detection. In *European Conference on Computer Vision*, pages 399–415. Springer, 2024. [2](#)
- [150] Zhixing Zhang, Bichen Wu, Xiaoyan Wang, Yaqiao Luo, Luxin Zhang, Yinan Zhao, Peter Vajda, Dimitris Metaxas, and Licheng Yu. Avid: Any-length video inpainting with diffusion model. In *IEEE Conf. Comput. Vis. Pattern Recognit.*, pages 7162–7172, 2024. [2](#)
- [151] Hanqing Zhao, Wenbo Zhou, Dongdong Chen, Tianyi Wei, Weiming Zhang, and Nenghai Yu. Multi-attentional deepfake detection. In *IEEE Conf. Comput. Vis. Pattern Recognit.*, pages 2185–2194, 2021. [3](#)
- [152] Wenliang Zhao, Yongming Rao, Weikang Shi, Zuyan Liu, Jie Zhou, and Jiwen Lu. Diffswap: High-fidelity and controllable face swapping via 3d-aware masked diffusion. In *IEEE Conf. Comput. Vis. Pattern Recognit.*, pages 8568–8577, 2023. [3](#)
- [153] Zangwei Zheng, Xiangyu Peng, Tianji Yang, Chenhui Shen, Shenggui Li, Hongxin Liu, Yukun Zhou, Tianyi Li, and Yang You. Open-sora: Democratizing efficient video production for all. *arXiv preprint arXiv:2412.20404*, 2024. [4](#), [5](#), [16](#), [17](#), [19](#)

- [154] Nan Zhong, Yiran Xu, Sheng Li, Zhenxing Qian, and Xinpeng Zhang. Patchcraft: Exploring texture patch for efficient ai-generated image detection. *arXiv preprint arXiv:2311.12397*, 2023. 2
- [155] Shangchen Zhou, Chongyi Li, Kelvin C.K Chan, and Chen Change Loy. ProPainter: Improving propagation and transformer for video inpainting. In *Int. Conf. Comput. Vis.*, 2023. 5, 16, 19
- [156] Yipin Zhou and Ser-Nam Lim. Joint audio-visual deepfake detection. In *Int. Conf. Comput. Vis.*, pages 14800–14809, 2021. 3
- [157] Yuan Zhou, Qiuyue Wang, Yuxuan Cai, and Huan Yang. Allegro: Open the black box of commercial-level video generation model. *arXiv preprint arXiv:2410.15458*, 2024. 3, 4, 5, 16, 17, 19
- [158] Jun-Yan Zhu, Taesung Park, Phillip Isola, and Alexei A. Efros. Unpaired image-to-image translation using cycle-consistent adversarial networks. In *Int. Conf. Comput. Vis.*, 2017. 2, 3
- [159] Mingjian Zhu, Hanting Chen, Qiangyu Yan, Xudong Huang, Guanyu Lin, Wei Li, Zhijun Tu, Hailin Hu, Jie Hu, and Yunhe Wang. Genimage: A million-scale benchmark for detecting ai-generated image. In *IEEE Conf. Comput. Vis. Pattern Recognit.*, 2023. 2
- [160] Bojia Zi, Minghao Chang, Jingjing Chen, Xingjun Ma, and Yu-Gang Jiang. Wilddeepfake: A challenging real-world dataset for deepfake detection. In *Proceedings of the 29th ACM International Conference on Multimedia (MM '21)*, 2021. 2
- [161] Bojia Zi, Shihao Zhao, Xianbiao Qi, Jianan Wang, Yukai Shi, Qianyu Chen, Bin Liang, Rong Xiao, Kam-Fai Wong, and Lei Zhang. Cococo: Improving text-guided video inpainting for better consistency, controllability and compatibility. In *AAAI Conf. Artif. Intell.*, pages 11067–11076, 2025. 2

A. Detailed Experiment Results

More detailed experiment results We present in Figure 8 and Table 6 the detailed statistics of our benchmark. We observe the following trends: (1) All OoB detectors exhibit consistently low performance, covering only a small area in the radar plots. (2) FoM methods demonstrate large performance variance: C2P [113] and D3 [143] perform very well, but predominantly on the Full-fake region (right half of the radar map). Both models, however, fail notably on Inpainting, especially the ROVI variant. (3) Within VLM-based detectors, only SIDA [56] shows partial effectiveness, again mainly on Full-fake generators. (4) For DiB, DRCT [16] achieves the most balanced performance across both Full-fake and fake-part categories, performing strongly on Inpainting, Change-of-Style, and several Faceswap cases. However, its notably weak result on Extrapolation (Cosmos), together with the fact that it rarely exceeds the very-high-performance range (above 85%), suggests that diffusion-based detectors still struggle to reach high-accuracy regimes. This indicates that even the best-performing DiB method leaves the overall detection problem posed by the FakePartsBench benchmark far from solved.

Analysis of the Most and Least Detectable Samples.

Figure 8 further highlights the challenge of detecting FakeParts manipulations by visualizing the distribution of the most- and least-detectable samples. The most-detected group (i.e., videos flagged by at least 12 detectors) is dominated by Full-Fake content—especially T2V—confirming that fully synthetic videos remain comparatively easy for detectors across all categories. In contrast, the least-detected samples show a strikingly different pattern: almost all are detected exclusively by DRCT [16] and missed entirely by every other detector. This reinforces our earlier finding that DRCT is the most balanced detector in the benchmark, capable of capturing subtle inconsistencies overlooked by others. Interestingly, these difficult cases span both Full-Fake and FakeParts examples, indicating that partial and localized manipulations continue to pose substantial challenges for most existing detectors. Figure 9 presents qualitative examples of both extremes. We see that many of the most-detected samples appear visually convincing, even to human observers, suggesting that strong detector performance does not necessarily correlate with human perceptual difficulty. This divergence between machine and human sensitivity underscores the need for deeper understanding of what cues different detectors rely on, especially in the presence of FakeParts artifacts.

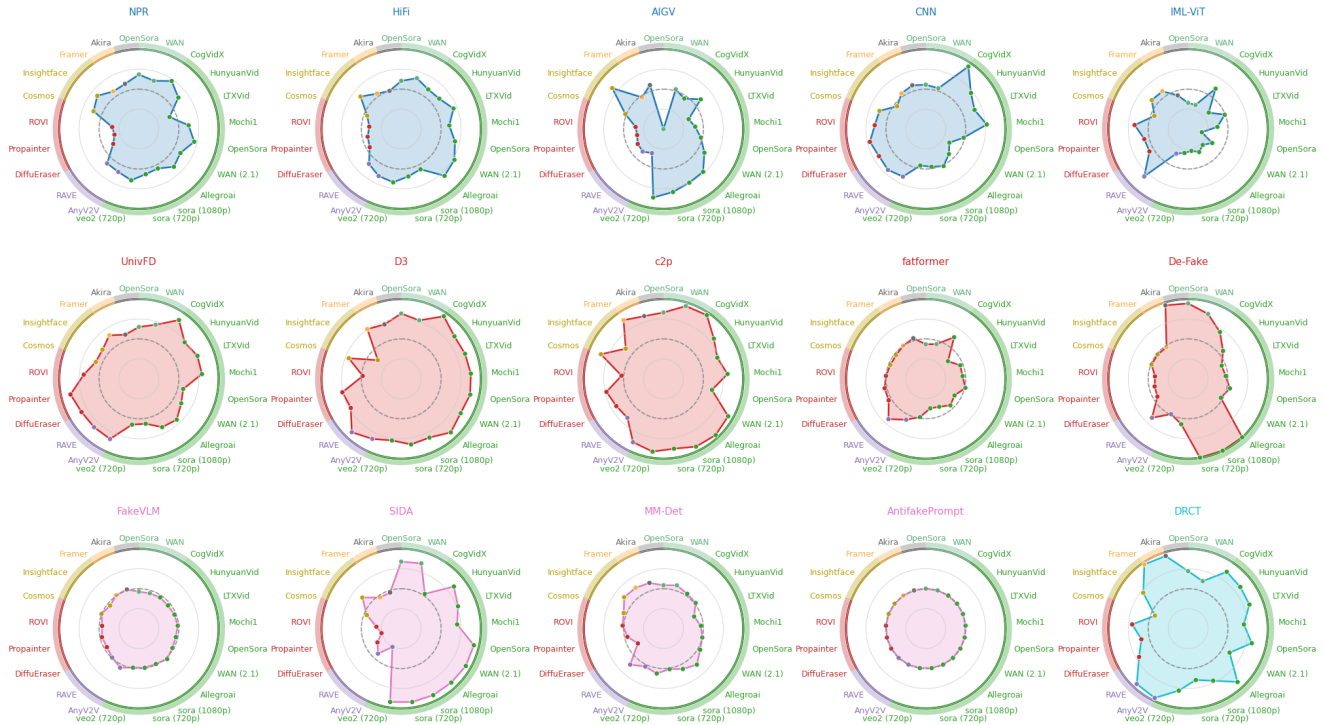


Figure 8. **Results** in Radar map of FakePartsBench performance across detector categories, where for each category we report the average performance achieved among all generators: **OoB**, **FoM**, **VLM**, and **DiB** and on various generators, including **full fake** generators such as: **T2V**, **Ti2V**, and FakeParts: **Change-of-Style**, **Inpainting**, **Outpainting**, **Interpolation**, **Extrapolation**, and **Faceswap**.

B. Generated Data Summary in FakeParts-Bench

The table 7 summarises the detailed statistics of both the generated and real data included in FakePartsBench. It provides an overview of all 21 methods covered in our benchmark, including *Style Change* [59, 66], *Extrapolation* [2, 34], *FaceSwap* [29], *Inpainting* [70, 136, 155], *Interpolation* [127], *Outpainting* [130], *T2V* [12, 23, 49, 64, 115, 120, 144, 153, 157], and *Ti2V* [120, 153]. For each method, we list the number of real and fake videos, the corresponding frame counts, and the native resolution, frame rate, and clip duration (or a range when applicable).

C. Extra information on the Human Perception Study

To rigorously assess the perceptual quality of the generated deepfake videos in our new benchmark, we developed a dedicated annotation platform to collect large-scale human judgments. This platform enables participants to watch each video and indicate whether they believe it is real or fake. After submitting their judgment, they are prompted to provide a short explanation justifying their decision. In total, **290** individuals participated in the annotation process, providing both binary classifications and qualitative feed-

back. Annotators interacted with a simple, intuitive UI that ensures both accessibility and consistency across evaluations. Metadata such as response times and annotator confidence levels were not collected to keep the privacy of annotators. After analysing the qualitative responses, we identified four recurring types of perceptual cues commonly cited by annotators when labelling videos as fake:

Human Rationales. We analyzed participant comments and found four recurring patterns:

1. **Temporal Inconsistencies:** unnatural transitions, jitter, or overly smooth motion.
2. **Facial and Body Artifacts:** misaligned expressions, inconsistent eye/lip movement, weird blending.
3. **Texture and Lighting Cues:** blurry details, mismatched lighting/shadows.
4. **Semantic Anomalies:** unrealistic object behavior, physics violations.

Implications. Human perception is strongly influenced by low-level visual cues and spatio-temporal coherence. To evade detection, generative models must improve:

- *Motion realism* (physically plausible dynamics),
- *Temporal consistency* (stable shadows and lighting),
- *High-frequency detail* (sharp but coherent textures).

Table 6. Performance comparison of video generators and detectors in terms of ROC-AUC (in %). Cells in green indicate scores $\geq 85\%$, while red cells indicate scores $\leq 53\%$. Detector columns are color-coded by family: **OoB**, **FoM**, **VLM**, and **DiB**. Generator rows are grouped by genre, including **full-fake** generators **T2V** and **TI2V**, as well as FakeParts manipulations such as **Change-of-Style**, **Inpainting**, **Outpainting**, **Interpolation**, **Extrapolation**, and **Faceswap**.

Generator	NPR	HiFi	AIGV	CNNDet	IML-ViT	UnivFD	D3	C2P	Fatfrm.	De-Fake	FakeVLM	SIDA	MM-Det	AFPrompt	DRCT
Random	50.0	50.0	50.0	50.0	50.0	50.0	50.0	50.0	50.0	50.0	50.0	50.0	50.0	50.0	50.0
OpenSora-768p	62.9	57.9	-	56.0	38.9	63.6	80.6	83.1	45.3	94.4	49.9	86.3	52.4	50.0	69.5
WAN	59.5	63.2	57.1	54.0	38.6	69.1	76.1	95.3	47.4	84.9	49.9	86.9	53.8	50.0	65.2
CogVidX	66.4	63.7	52.2	94.5	55.2	86.3	91.0	97.3	57.9	68.4	49.4	53.8	51.4	50.0	83.0
HunyuanVid	59.4	56.2	68.3	75.9	40.8	74.2	83.1	84.1	42.1	57.5	49.7	85.3	50.9	50.0	84.0
LTXVid	42.9	70.9	44.6	64.4	48.4	76.1	85.8	77.1	47.4	46.7	49.3	76.0	45.2	50.0	83.0
Mochi1	59.0	57.8	45.8	73.6	41.0	79.0	86.6	83.2	47.5	47.9	49.5	74.0	48.0	50.0	66.8
OpenSora	64.5	64.4	56.5	49.0	34.4	56.6	88.6	63.4	49.5	53.6	49.4	94.3	49.8	50.0	81.1
WAN (2.1)	56.2	74.2	63.0	39.3	39.7	58.9	86.5	93.7	44.3	48.1	49.4	94.0	51.7	50.0	63.5
Allegroai	59.6	76.9	71.8	43.9	36.7	67.6	91.5	96.5	47.2	99.8	51.2	92.9	56.6	50.0	91.9
sora (1080p)	53.2	52.9	74.7	51.0	38.4	65.2	81.7	94.5	42.6	99.8	49.6	93.2	53.5	50.0	73.8
sora (720p)	54.7	56.6	79.9	48.4	36.9	55.5	82.9	89.3	41.8	99.7	49.8	93.6	50.7	50.0	69.1
veo2 (720p)	60.0	63.8	86.2	45.1	38.0	56.8	79.1	92.2	49.3	65.1	49.8	93.4	53.9	50.0	75.1
AnyV2V	56.6	61.4	43.6	64.5	40.0	83.2	85.2	90.7	56.3	49.0	52.9	38.2	51.3	50.0	96.3
RAVE	55.7	57.5	41.9	65.5	82.1	81.0	89.4	73.7	64.5	66.1	49.7	49.1	56.6	50.0	95.1
DiffuEraser	41.0	46.7	46.8	65.5	53.7	80.6	72.7	72.6	51.6	45.1	49.8	39.9	42.7	50.0	68.4
Propainter	38.1	45.2	42.7	71.8	53.8	88.5	76.3	79.4	51.0	44.2	49.3	36.2	47.9	50.0	56.6
ROVI	39.5	42.7	44.4	62.8	61.3	68.6	50.4	58.5	48.7	43.8	49.9	38.2	50.8	50.0	68.2
Cosmos	75.6	65.7	55.3	76.9	67.5	75.5	84.4	91.7	67.9	68.9	69.3	66.7	51.9	69.1	81.9
Insightface	68.3	65.4	84.6	53.0	62.8	60.5	51.2	64.6	58.0	61.4	58.1	66.0	57.5	58.2	65.9
Framer	34.3	32.3	50.1	32.9	34.8	45.6	60.1	81.1	30.5	29.2	30.7	29.2	56.9	30.4	95.3
Akira	56.1	49.2	65.3	55.2	45.9	56.4	71.9	84.3	52.3	96.7	50.7	48.4	55.6	50.0	95.1



Figure 9. **Demonstrations** of the least and most detectable generated samples. The **first row** shows four *least detected* examples, identified **only** by DRCT [16] and missed by all other detectors. The **second row** presents the *most detected* examples, each correctly flagged by **more than 12 detectors**. A clear pattern emerges: highly detectable cases are predominantly **full-fake videos**, whereas the most challenging cases are almost exclusively **FakeParts** samples.

D. Implementation details

I. Full Deepfakes The Full Deepfake category in FakeParts includes two types: Text-to-Video (T2V) and Text-and-Image-to-Video (IT2V).

Text-to-Video (T2V). For T2V, we include a range of open-source generators, such as CogVideoX [144], Hunyuan Video [64], LTX-Video [49], Mochi 1 by Genmo [115], Open-Sora [153], Wan2.1 [120], and AllegroAI [157], as well as commercial generators Sora [12] and Veo2 [23], all released between 2024 and 2025. To ensure diverse and semantically rich content, we generate prompts for all T2V methods using Google Gemini [116].

Text-and-Image-to-Video (IT2V). For IT2V, we include

models that support dual-modality conditioning (text and image), such as Open-Sora [153] and Wan2.1 [120]. We first extract the initial frame from real videos (e.g., from Pexels [86]) and then query a VLM (Gemini) to produce a continuation prompt conditioned on this frame. Both the prompts and the corresponding conditioning frames will be included in our metadata.

II. FakeParts

Spatial FakeParts In the spatial subset of FakeParts, we focus on methods that alter regional information within the video content.

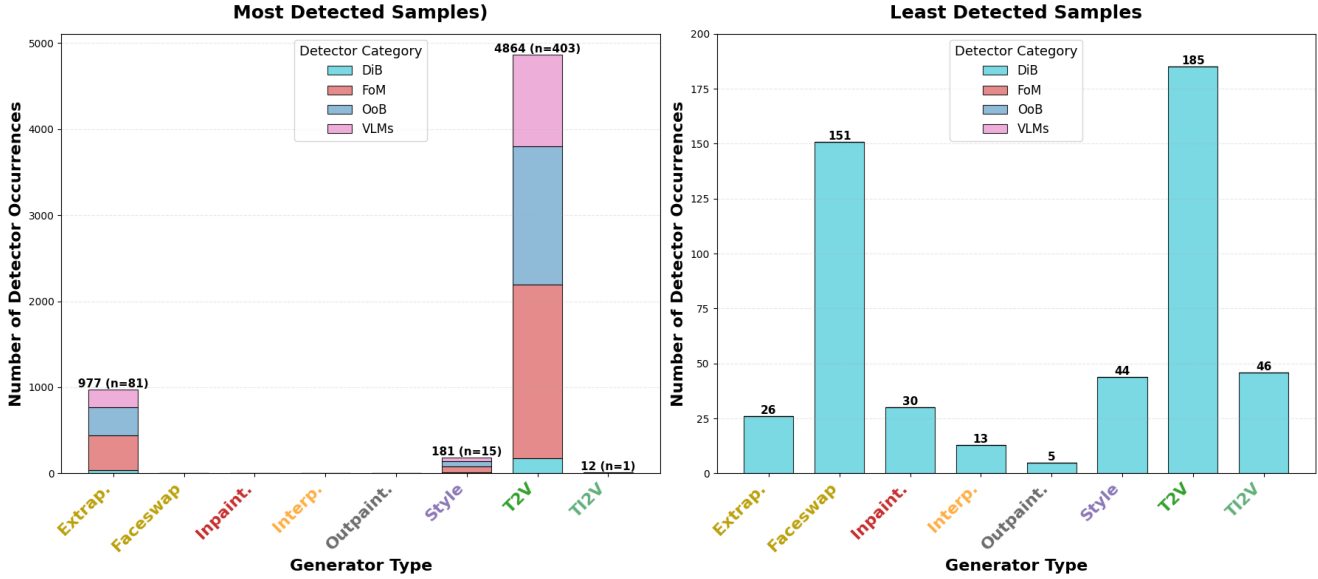


Figure 10. **Histogram** of the least and most detectable generated samples. We sample 500 of the most-detected and 500 of the least-detected videos and collect their occurrences (note that we have 15 detectors). For the most-detected group, the vast majority are Full-Fakes, especially T2V generations. In contrast, the least-detected samples are almost exclusively detected by a single detector, DRCT [16], and missed by all others, consistent with our observation that DRCT is the most balanced detector. Moreover, these least-detected examples span both Full-Fakes and FakeParts, further highlighting our finding that partial manipulations are significantly harder for most detectors.

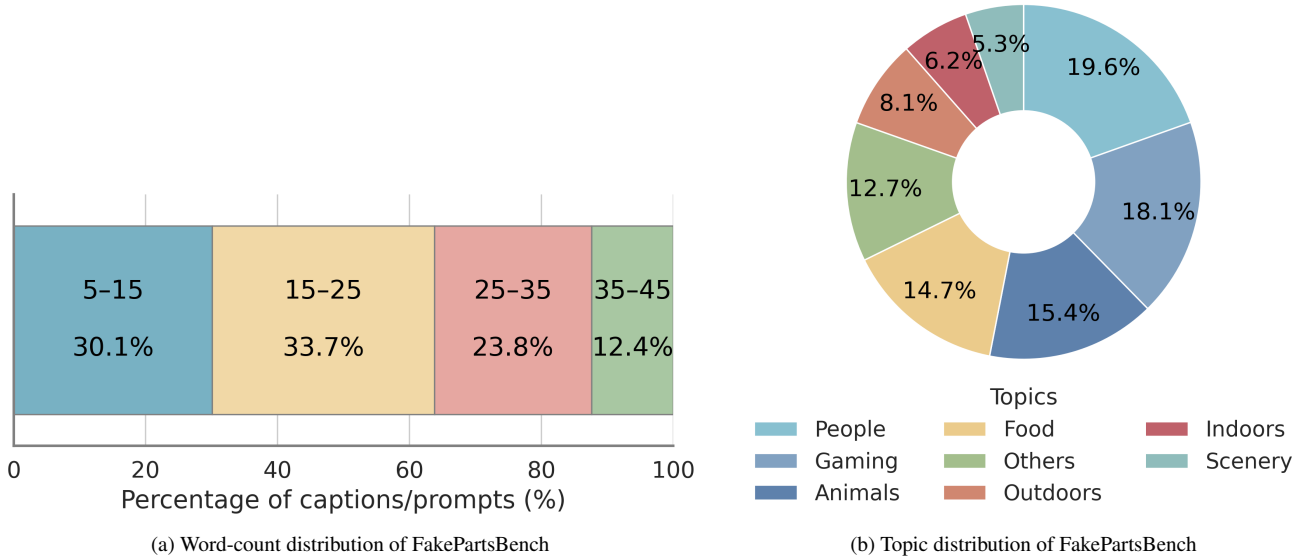


Figure 11. The distribution in terms of the caption length and theme category of the generated video content in our FakePartsBench.

FaceSwap Generation. To create FaceSwap deepfakes, we replaced the face in a target video with that from a source face image. This was achieved using the InsightFace library [3, 4, 28–31, 39, 44, 45, 99], a widely used tool for face detection and swapping. Given the special requirement of the facial information in the video we draw our target videos from Celeb-DF dataset [73] and source ones from the

CelebA dataset [79] and an additional set of celebrity face images collected in 2022. To ensure gender consistency between the source and target frames, we prompt VLM with: "What is the gender of the person in the image?" and filter the unmatched pairs.

Inpainting Generation. Inpainting-based manipulations simulate object removal within video scenes. We include

Table 7. Detailed statistics for all methods.

Year	Venue	Task	Method	RealV	FakeV	TotV	RealF	FakeF	TotF	Resolutions	FPS	Dur
2024	TMLR 2024	Style Change	AnyV2V [66]	0	1,545	1,545	0	24,720	24,720	512×512	8	2
2023	CVPR 2024	Style Change	RAVE [59]	0	3,721	3,721	0	487,476	487,476	680×384	10	14
2025	arXiv	Extrapolation	Cosmos-Predict2 [2]	120,000	3,000	3,000	120,000	268,618	388,618	1280×704	25	5
2019	CVPR 2019	Faceswap	InsightFace [29]	0	5,036	5,036	0	1,990,470	1,990,470	—	30	11
2025	arXiv	Inpainting	DiffuEraser [70]	0	2,243	2,243	0	75,871	75,871	1280×720	6	6
2023	ICCV 2023	Inpainting	ProPainter [155]	0	2,244	2,244	0	75,907	75,907	1280×720	6	6
2024	CVPR 2024	Inpainting	ROVI [136]	7,252	9,090	9,090	16,342	199,032	247,014	426×320–1280×720	5	4
2025	ICLR 2025	Interpolation	Framer [127]	320,000	10,000	10,000	320,000	140,000	460,000	512×320	7	7
2025	CVPR 2025	Outpainting	Akira [130]	0	7,275	7,275	0	101,850	101,850	576×320	8	2
2025	ICLR	T2V	CogVideoX [144]	0	2,720	2,720	0	377,629	377,629	720×480	25	5
2024	arXiv	T2V	HunyuanVideo [64]	0	1,550	1,550	0	109,646	109,646	1280×720	15	4
2024	arXiv	T2V	LTXVideo [49]	0	2,605	2,605	0	365,629	365,629	1280×720	30	5
2024	Report	T2V	Mochi1 [115]	0	1,059	1,059	0	137,367	137,367	848×480	25	5
2024	arXiv	T2V	Open-Sora [153]	0	2,000	2,000	0	258,000	258,000	1024×576	24	5
2025	arXiv	T2V	Wan (2.1) [120]	0	1,423	1,423	0	115,263	115,263	1280×720	16	5
2024	arXiv	T2V	allegroai [157]	0	1,000	1,000	0	88,000	88,000	1280×720	15	6
2025	OpenAI Report	T2V	sora-1080p [12]	0	997	997	0	148,871	148,871	1920×1080	30	5
2025	OpenAI Report	T2V	sora-720p [12]	0	1,766	1,766	0	264,900	264,900	1280×720	30	5
2024	Google Report	T2V	veo2-720p [23]	0	999	999	0	119,880	119,880	1280×720	24	5
2024	arXiv	T12V	Open-Sora-768px [153]	0	1,980	1,980	0	255,420	255,420	1024×576	24	5
2025	arXiv	T12V	WAN [120]	0	2,000	2,000	0	162,000	162,000	720×1280	16	5
–	–	Real	TenKReal	10,000	0	10,000	1,428,515	0	1,428,515	640×360	30	6
ALL	–	–	–	17,252	64,252	81,504	2,067,507	5,814,442	7,881,949	–	–	–

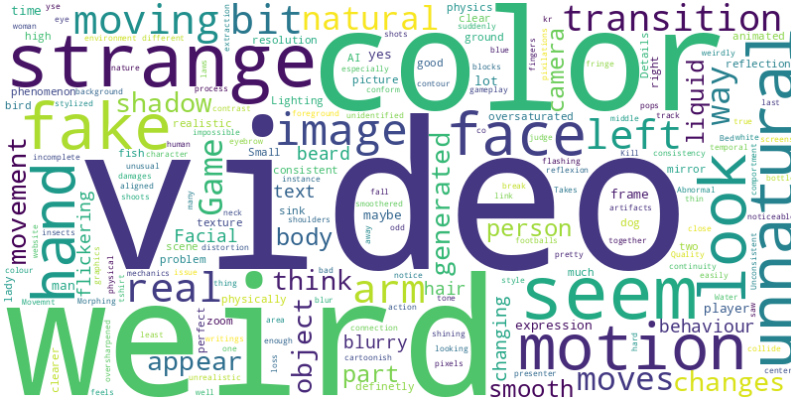


Figure 12. Word cloud showing the most frequent terms from human explanations of synthetic content detection.

two sources of inpainted videos.

First, we generate new inpainted FakeParts using two recent video inpainting methods, DiffuEraser [70] and ProPainter [155]:

1. we extract the first frame from each video and query a vision-language model (VLM) with the prompt “What is one interesting object in the image that is neither too

small to be noticeable nor so large that it occupies almost the entire frame?” to identify a salient object for removal;

2. we segment the selected object across all frames using Grounded-SAM-2 [97], obtaining a temporally consistent mask;
3. we apply DiffuEraser or ProPainter to remove the object



Figure 13. Examples of real videos collected from YouTube-VOS 2019 [142].

and fill the masked regions, producing realistic object-removal deepfakes.

Second, we incorporate the language-driven inpainting dataset from ROVI [136], where videos are inpainted using E2FGVI [136] under carefully curated prompts and parameter settings. These ROVI inpainted clips are included as part of our inpainting FakeParts, complementing our own DiffuEraser/ProPainter-based generations with an additional, independently constructed inpainting pipeline.

Outpainting. Unlike mainstream image inpainting and outpainting methods [5, 80], which primarily extrapolate content beyond image boundaries, video outpainting introduces additional complexities related to camera motion and 3D scene consistency. Recent methods address this by explicitly integrating camera control into video generation [51, 130, 134, 139]. In this section, we adopt the AkiRA model [130], built upon the SVD framework [10], which generates video content consistent with specified camera trajectories. Specifically, we apply backwards camera tracking as conditioning input, enabling coherent extrapolation at frame boundaries.

Temporal FakeParts In the temporal subset of FakeParts, we focus on methods that complete or modify content along the time axis, such as frame interpolation.

Interpolation Generation. For interpolation-based manipulations, we employ the Framer model [127] to synthesize smooth transitions between non-consecutive frames, simulating temporal manipulations. From each source video the first and last frames are provided to Framer, which generates 21 intermediate frames to fill the temporal gaps and produce a temporally manipulated video sequence.

Extrapolation Generation. To generate temporally extrapolated videos, we employ the Cosmos Predict

Video2World framework [2, 34], which predicts future motion and scene evolution. Given the final 50 frames of a captured sequence, together with their caption as prompt, the model synthesises subsequent frames to extend each clip to 120 frames. The resulting 25 FPS, 5-second videos preserve the original scene context while introducing plausible forward dynamics, forming our extrapolation subset.

Style FakeParts The style subset of FakeParts targets manipulations that retain the semantic content of the video but modify its appearance through style transfer techniques.

Style Change Generation. We use the diffusion-based RAVE model [59] to alter the colour and appearance of animals in videos from the Animal Kingdom dataset [87]. For each video, we randomly sample a frame, caption it using PaLI-Gemma 2 [110], and prompt RAVE with: “Change the colour of the animal in the video.” In addition, we include object-specific colour edits generated with AnyV2V [66]. In this case, frames are first captioned with VideoChat-R1 [71], from which we identify the object to edit and a target colour description. We then construct prompts such as “Change the colour of the car to blue while keeping the rest of the scene unchanged.”, ensuring that only local appearance is modified while preserving global scene semantics.

E. Metadata to be Released

We will release all metadata necessary to reproduce each generation task in our study. All metadata will be uploaded together with the dataset to our public HuggingFace repository.



A young woman in a white dress walks through a lush, green forest, pausing to admire vibrant flowers. The camera pans to a serene lake, where a family of ducks swims. The scene shifts to a cozy cabin nestled among the trees, with smoke rising from the chimney. The woman sits on a bench, gazing out at the landscape.



A person examines and handles a collection of trading cards, sorting through and interacting with the various cards featuring diverse designs and characters.



A character in a black and pink outfit with a yellow helmet rides a pink motorcycle with black accents on a green ramp with "SPRUNK" written on it. The character launches the motorcycle off the ramp, performing a mid-air stunt, and lands back on the ramp. The background shows a body of water with a rocky shoreline under clear skies.



A person slices a bread-like item on a cutting board with a knife in a kitchen. Bowls are visible in the background. The overhead camera angle shows the action in a brightly lit kitchen setting.



A person wearing a light blue shirt works on a wall, handling a long, narrow object, possibly a piece of wood. The camera focuses on their hands and the object as they perform a series of actions. The background remains simple. The person's hands are shown handling the object, making changes to its condition, and installing or completing the task.



A bearded man in a gray jacket and blue jeans stands in a curved, tunnel-like space with a rope or cable running along the wall. He looks straight ahead, then down, and finally tilts his head.

Figure 14. Examples of **Full Fakes**, including T2V (first two rows from SoRA [12] and second two rows are from Veo2 [23]) and IT2V from SoRA [12]. Green strokes indicate the condition image used in IT2V.

Metadata for T2V Generation For the text-to-video (T2V) generation task, we provide the full set of textual prompts used as model inputs.

- **Format:** CSV

- **Fields:**

- id
- prompt_text

Metadata for TI2V Generation For the text-and-image-to-video (TI2V) generation task, we provide all multimodal prompts used in the experiments.

- **Format:** CSV

- **Fields:**

- id
- prompt_text
- image_reference (reference to the corresponding input image)

Metadata for Real Videos Used in Extrapolation For real videos used as the basis for the Extrapolation task, we provide structural video clips' metadata and aligned captions.

- **Format:** CSV

- **Fields:**

- name
- fps

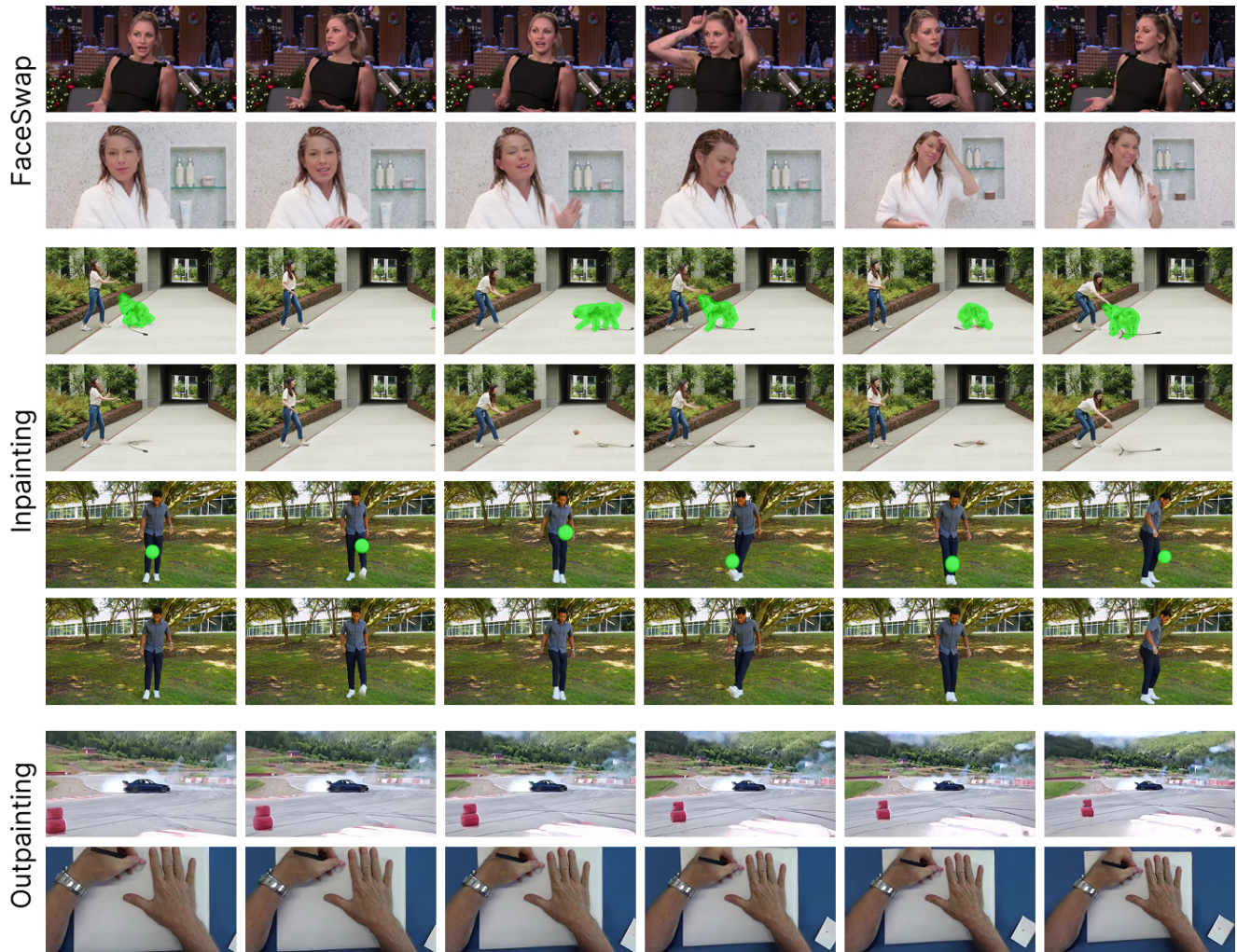


Figure 15. Examples of **Spatial FakeParts**, including FaceSwap, inpainting, and outpainting methods. In inpainting, the green mask indicates the region to be removed.

- width
- height
- caption

Metadata for Real Videos Used in Style Change For real videos used as style sources in the Style Change task, we release their corresponding metadata, captions and object concerned.

- **Format:** CSV
- **Fields:**
 - name
 - fps
 - width
 - height
 - caption
 - objects

Metadata for Extrapolation and Style-Change Prompts

We additionally release the prompt format and pipelines used specifically for the Extrapolation and Style-Change generation tasks.

- **Format:** Jupyter Notebook

Release Format and Location All metadata will be released in CSV format and hosted within the same Hugging-Face dataset repository as the main data, ensuring full reproducibility.

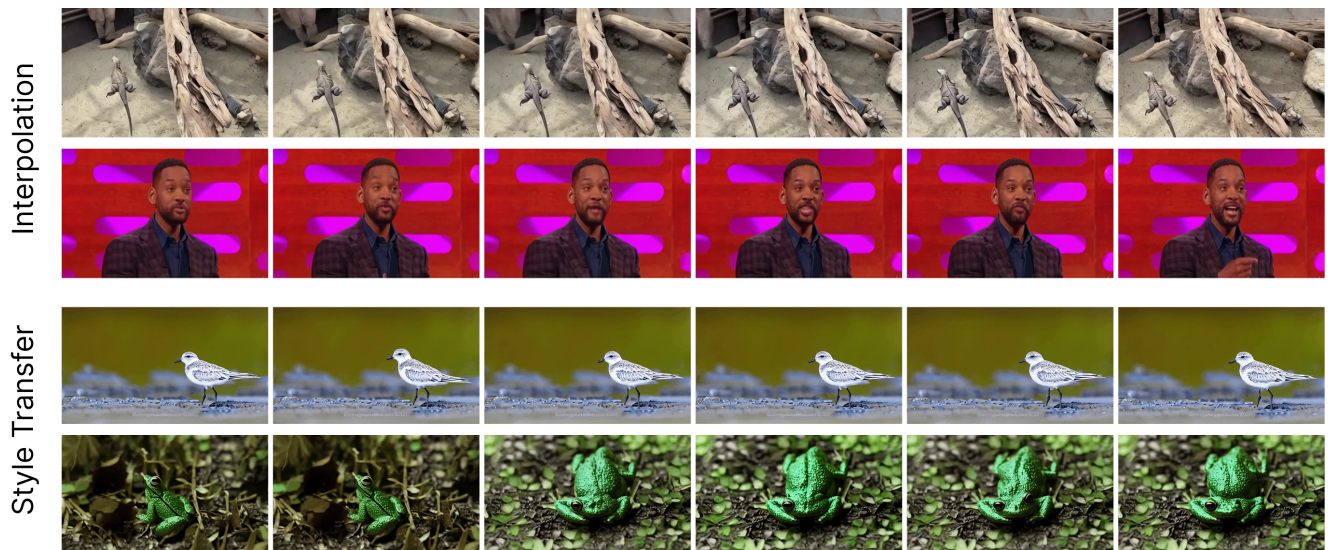


Figure 16. Examples of **Temporal and Style FakeParts**, including Frame interpolation and Style Transfer.